

Article

CRISPR/Cas9 deletions in a conserved exon of *Distal-less* generates gains and losses in a recently acquired morphological novelty in flies

Gowri Rajaratnam,
Ahiraa
Supeinthiran,
Rudolf Meier,
Kathy F.Y. Su

meier@nus.edu.sg (R.M.)
kathysufy@gmail.com
(K.F.Y.S.)

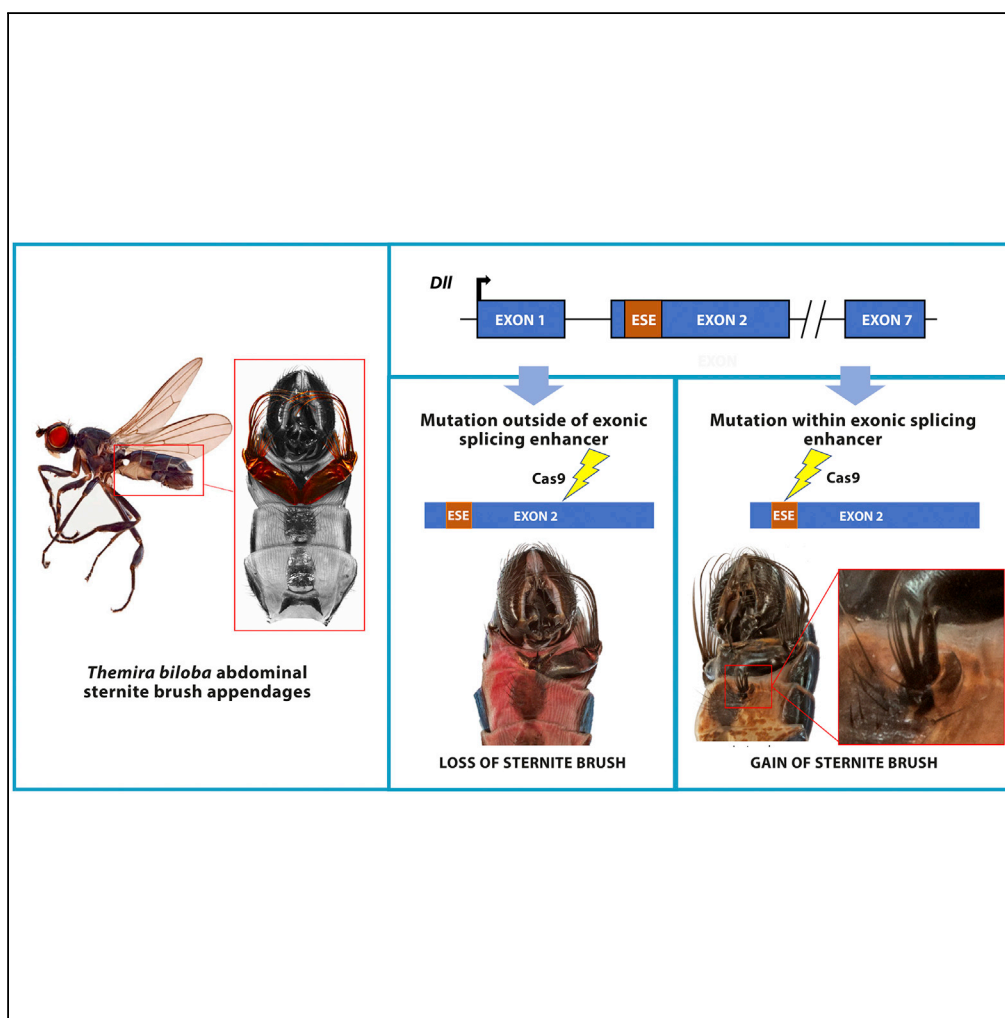
HIGHLIGHTS

Distal-less is necessary for the development of a novel abdominal appendage

CRISPR/Cas9 editing produced both losses and gains of novel abdominal appendages

Gains of appendages result from mutations in exonic splicing enhancer (ESEs) sites

ESE mutations likely led to exon skipping and an altered *Distal-less* protein



Article

CRISPR/Cas9 deletions in a conserved exon of *Distal-less* generates gains and losses in a recently acquired morphological novelty in fliesGowri Rajaratnam,¹ Ahiraa Supeinthiran,³ Rudolf Meier,^{1,2,*} and Kathy F.Y. Su^{1,4,*}

SUMMARY

Distal-less has been repeatedly co-opted for the development of many novel traits. Here, we document its curious role in the development of a novel abdominal appendage (“sternite brushes”) in sepsid flies. CRISPR/Cas9 deletions in the homeodomain result in losses of sternite brushes, demonstrating that *Distal-less* is necessary for their development. However, deletions in the upstream coding exon (Exon 2) produce losses or gains of brushes. A dissection of Exon 2 reveals that the likely mechanism for gains involves a deletion in an exon-splicing enhancer site that leads to exon skipping. Such contradictory phenotypes are also observed in butterflies, suggesting that mutations in the conserved upstream regions have the potential to generate phenotypic variability in insects that diverged 300 million years ago. Our results demonstrate the importance of *Distal-less* for the development of a novel abdominal appendage in insects and highlight how site-specific mutations in the same exon can produce contradictory phenotypes.

INTRODUCTION

Insects display a remarkable amount of morphological diversity. Such diversity can be generated through the co-option of existing gene modules in novel environments. One such repeatedly co-opted gene is *Distal-less* (*Dll*), which codes for a transcription factor that is essential for insect appendage patterning. *Dll* has been shown to be involved in the development of many morphological novelties that are essentially distal cuticular projections, like the grasping structures on antenna in male water striders (Khila et al., 2012), the nasus in termites (Toga et al., 2012), and the thoracic horns in scarab beetles (Moczek and Rose, 2009). *Dll* has even been co-opted for the development of novel pigmentation patterns in the wings of flies (Arnoult et al., 2013) and eyespots in butterflies (Zhang and Reed, 2016). Here, we look at its role in the development and evolution of another morphological novelty, an abdominal sternite brush in sepsids.

Males of some sepsid species (Sepsidae: Diptera) have evolved a moveable appendage on their fourth abdominal segment, the fourth sternite brush (Figure 1A). This novel appendage in sepsids is a modification of a sternite plate on the ventral fourth abdominal segment. In some species, the fourth sternite has been dramatically modified into a large, sclerotized leg-like structure that is complete with underlying musculature, articulation, and long distal brushes (Ang, 2013). Male sepsids use these elaborate appendages to stimulate females during copulation (Figure 1B, <https://www.youtube.com/watch?v=BL9wffTKO50&feature=youtu.be>). The fourth sternite brushes range from simple flat plates with few bristles to highly elaborate appendages (Figure 1C). A phylogenetic analysis reveals that the fourth sternite brush has a complex evolutionary history. It was acquired early in the radiation of this family, then lost multiple times, and then reacquired at least once (Bowsher et al., 2013).

These structures also have an interesting developmental origin. Unlike typical dipteran appendages (e.g., legs and wings) that develop from imaginal discs, the novel sternite brush appendage in male sepsids develops from a cluster of ventral histoblast cells (Bowsher and Nijhout, 2007). In flies, histoblasts are clumps of imaginal cells that proliferate to form the adult abdominal epidermis, including the sternites and tergites. An earlier study characterized the expression pattern of *Dll* late in sepsid pupal development; they found that *Dll* was expressed only in the bristle cell nuclei of late-stage pupal tissues that give rise to the fourth sternite brush (Bowsher and Nijhout, 2009). Here, we develop and use CRISPR/Cas9 to show that *Dll* is involved in the development of these novel abdominal appendages in a non-model dipteran species, *Themira biloba* (Figure 1A). This is the first functionally characterized gene in a gene regulatory network involved in the development and evolution of a novel abdominal appendage. In the process, we discover

¹Department of Biological Sciences, National University of Singapore, Singapore, Singapore

²Lee Kong Chian Natural History Museum, Singapore, Singapore

³University of Toronto Scarborough, Toronto, Canada

⁴Lead Contact

*Correspondence: meier@nus.edu.sg (R.M.), kathysufy@gmail.com (K.F.Y.S.)

<https://doi.org/10.1016/j.isci.2018.11.036>



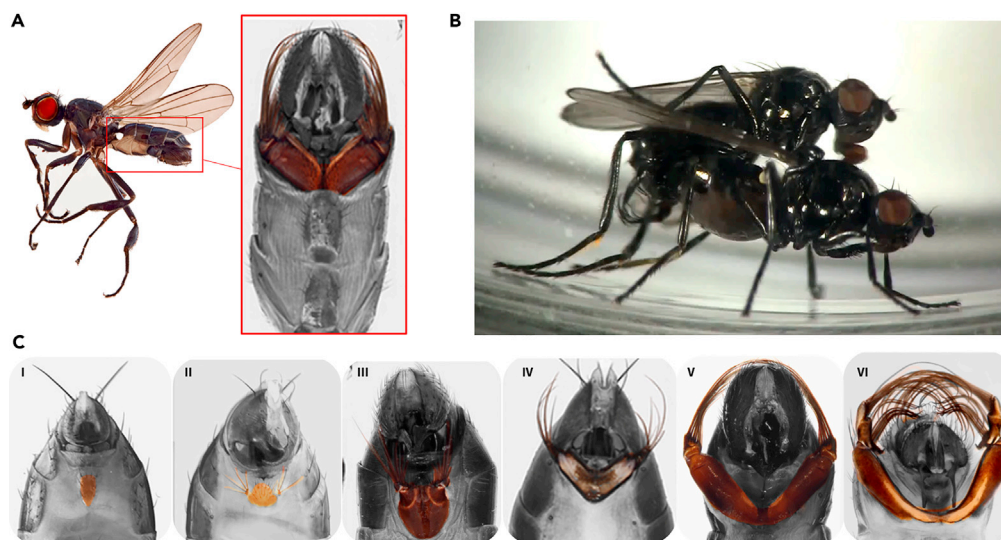


Figure 1. Sepsid Males of Some Species Have a Novel Appendage on Their Fourth Abdominal Segment Which Is a Modified Fourth Sternite (“Sternite Brush”)

(A–C) (A) Sternite brush of *Themira biloba* (highlighted in color). (B) Male *Themira superba* using the sternite brush to stimulate a female during mating. (C) Sternite diversity across Sepsidae: (i) *Dicranosepsis bicolor* without sternite modification and brushes in (ii) *Microsepsis armillata*, (iii) *Themira flavicoxa*, (iv) *Perochaeta dikowi*, (v) *Themira putris*, and (vi) *Themira superba*.

an interesting phenomenon wherein deletions in a conserved *Dll*-coding region generated via CRISPR/Cas 9 produced not only the expected losses but also gains of novel appendages on different abdominal segments.

RESULTS

Genome Editing at the *Dll* Locus Generates Loss-of-Function Mosaic Phenotypes

We designed three guides targeting two different exons within the *Dll* locus: the homeodomain (Exon 3) and the coding exon upstream of the homeodomain (Exon 2) (Figure 2A, Table S6). We screened for potential off-targets by conducting a local BLASTN search comparing the transcriptome of *T. biloba* (Melicher et al., 2014) against the three guide sequences.

We injected 4-hr-old *T. biloba* embryos with Cas9 protein and guides targeting these coding regions. We observe that *Dll* loss-of-function mutations are highly lethal; this result is similar to what has been shown in *Drosophila melanogaster* (Cohen and Jürgens, 1989). After optimization, we find that 20%–30% of embryos survive microinjection with 22%–37% of larvae developing into adults. In total, we obtained 80 mosaic mutants (Table 1). A total of 58 mutants were observed with malformed or missing sternites; monomorphic sternite malformations were observed in both males and females. However, sternite losses were only observed in males. We observed a higher proportion of abdominal or posterior phenotypes; this is likely due to the injection of CRISPR/Cas9 and single guide RNA (sgRNA) complex into the posterior end of the embryo. Even so, one in eight of the recovered mutants exhibited leg or wing phenotypes consistent with known *Dll* mutants in *D. melanogaster*: mosaic mutants with wing margin deformities, hindleg deformities, and loss of tarsal structures were observed (Figures 2B and 2C). All mutants were successfully verified with next-generation sequencing (NGS) on an Illumina MiSeq 2 x 300-bp platform with tagged amplicon sequencing (7-bp tags). The read counts and three most abundant mutant haplotypes for each mutant specimen can be found in Table S3. Only the most abundant mutant haplotype for each specimen was used for downstream alignments and analyses.

As a control, we injected approximately 1,000 embryos with Cas9 alone without obtaining mutant phenotypes (Table 1). The surviving adults from the control injections were genotyped through sequencing with NGS and found to have no mutations in the *Dll*-coding region. We also sequenced injected individuals displaying a wild-type phenotype and found no mutations in the *Dll*-coding region.

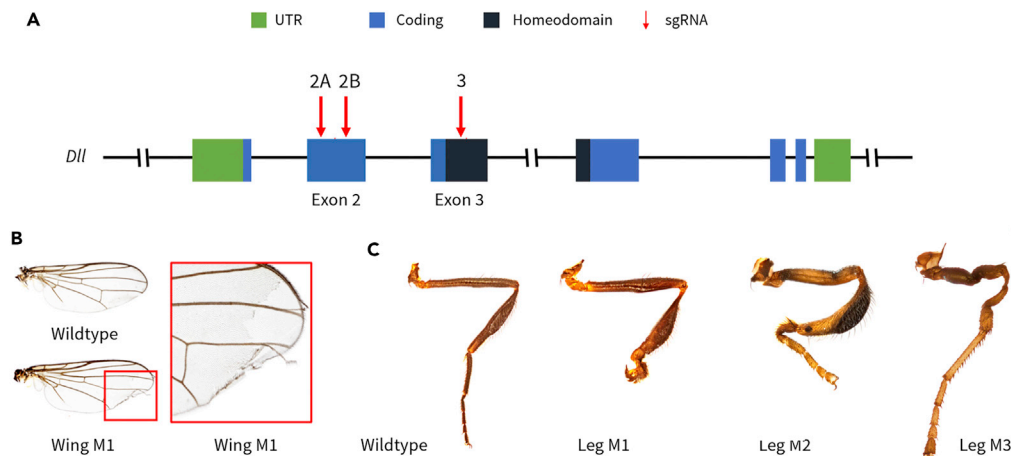


Figure 2. Deletions in *Dll*-Coding Region Generate Leg and Wing Mutants

(A–C) (A) The Homeodomain (Exon 3) and upstream coding exon (Exon 2) of *Dll* were targeted using CRISPR/Cas9. Three guides were designed: two within the coding regions of Exon 2 and one within the coding region of Exon 3. (B) Mosaic mutant with a disrupted wing margin (Exon 2, sgRNA-2B mutant). (C) Mosaic mutant males with leg deformations (Leg M1 and M2: Exon 2 sgRNA-2B mutants, Leg M3: Exon 3 mutant)

A Functional *Dll* Homeodomain Is Necessary for Fourth Sternite Brush Development

Targeted genome editing at the *Dll* homeodomain produced mosaic mutant males with loss of the fourth sternite appendage. The fourth sternite appendage in *T. biloba* consists of a bifurcated sternite with a pair of cuticular protrusions or lobes that each terminate in a tuft of bristles. Of the 21 mosaic mutants with sternite malformations, five exhibited malformed or missing fourth sternite appendages (Figure 3C): mutants E3 M1 and E3 M3 display a complete loss of the sternite, lobe, and bristles in one-half of the fourth sternite appendage, whereas in the others (E3 M2, E3 M4, and E3 M5) the lobe and bristles of one-half of the fourth sternite appendage were lost, leaving behind small misshapen remnants of the sternite. Characterization of these mutants with NGS showed deletions in the target region, which disrupted the reading frame (Figure 3B). These mosaic mutant phenotypes confirm that a functional *Dll* gene product is necessary for the development of this appendage in *T. biloba* males.

Genome Editing at the Coding Exon Upstream of the Homeodomain Produces Ectopic Structures

Targeting Exon 2, using sgRNA-2B, which is immediately upstream of the homeodomain, produced mosaic mutants with sternite malformations as expected (Figure S1). However, we also recover unexpected mutant males with small ectopic sternite brushes on the third ventral segment (Figure 4A) and the fourth dorsal segment (Figures 4B and 4C). In mutant E2B M1, we observed a small cuticular protrusion with a tuft of bristles on the top right margin of the third ventral sternite (Figure 4A). A similar ectopic cuticular protrusion with bristles was also observed in E2B M2 and E2B M3, wherein the protrusion disrupts the right margin of

	Injected Eggs	Larvae	Adults	Mutants			
				Leg/Wing	Sternite Malformations	Ectopic Structures	Others (e.g., Clasper Malformations)
Exon 2 (sgRNA 2A)	1,715	605	151	1	8	1	0
Exon 2 (sgRNA 2B)	4,631	957	363	8	29	3	6
Exon 3 (sgRNA3)	4,003	1,187	261	1	21	0	2
Control	1,004	153	109	0	0	0	0

Table 1. Summary of CRISPR/Cas9 Injection Results

Control injections were carried out using only Cas9 protein without any sgRNA.

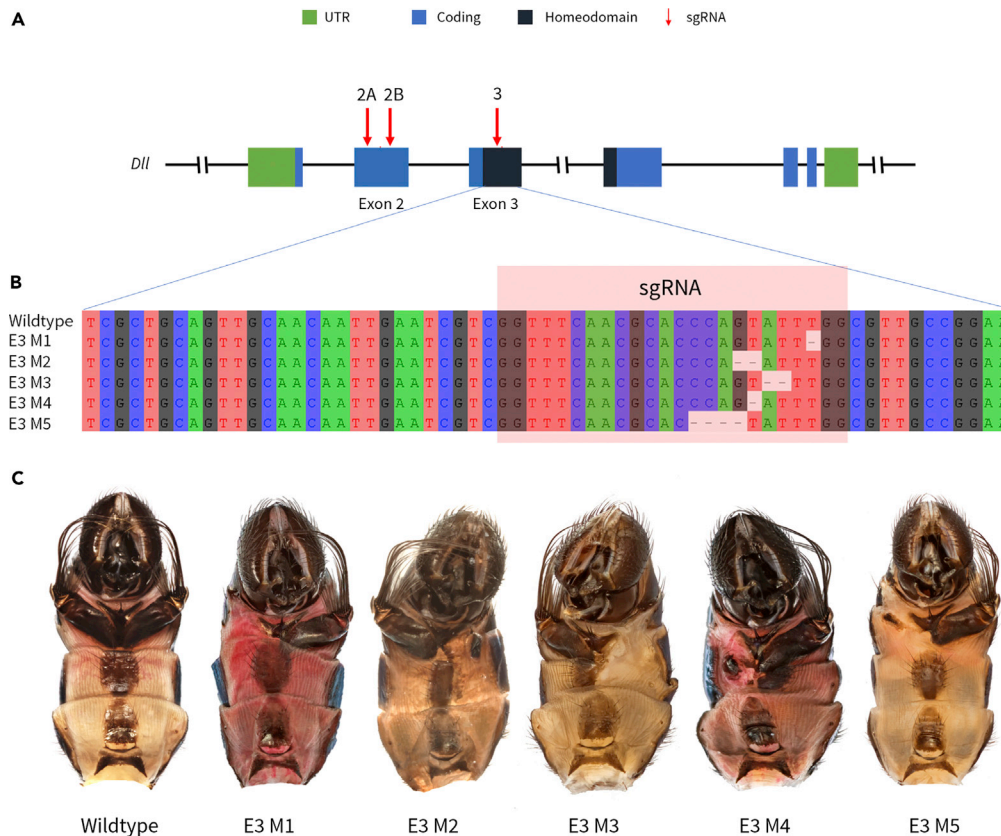


Figure 3. *Dll* Homeodomain Is Necessary for the Development of the Fourth Sternite Brush

(A) *Dll* locus.

(B) Disruptive mutations of Exon 3 yielding mosaic mutants in (C).

(C) Corresponding mosaic mutants with losses of the fourth sternite brush.

the fourth tergite (Figures 4B and 4C). To rule out the possibility that the ectopic phenotypes were a result of off-target gene editing, we screened for potential off-target effects (see Methods and Table S2 for additional details) and found no good matches (>65% identity).

Such exon-specific gain and loss phenotypes have similarly been observed in Lepidoptera wherein deletions in the *Dll* homeodomain result in losses of eyespots in *Bicyclus anynana* (Connahs et al., 2017), whereas deletions in the region upstream of the homeodomain can produce ectopic eyespots in *B. anynana* (Connahs et al., 2017) and *Vanessa cardui* (Zhang and Reed, 2016) as well as enlarged eyespots in *Junonia coenia* (Zhang and Reed, 2016). Comparative sequence analysis between Lepidoptera and Diptera reveals that this region of *Dll* is almost as highly conserved as the *Dll* functional homeodomain. Further investigation shows that it is conserved even across Holometabola (Figure S2).

To understand the genetic mechanism underlying the development of the ectopic brush phenotype, we sequenced all mosaic mutants using NGS. We find that a single point mutation underlies all ectopic mutant phenotypes (Figure 4D). A bioinformatics analysis of Exon 2 using ESEfinder 3.0 (Cartegni et al., 2003) revealed that this single point mutation lies within a predicted exonic splicing enhancer (ESE) site for the SR protein, splicing factor 2 (SF2) (Table S1). SF2 is an RNA-binding, sequence-specific splice factor that binds to ESE sites to promote inclusion of the exon during alternative splicing at the pre-mRNA level. In contrast, all other mutant phenotypes observed were due to mutations that lie outside of this predicted ESE site (Figure 4D). Previous studies of naturally occurring and artificially induced mutations in ESEs have shown that such mutations can lead to exon skipping (Hong-Xiang et al., 2001; Wang et al., 2002). This naturally occurring form of cellular RNA splicing occurs when defective portions of exons are “skipped” over to restore the reading frame. This produces an altered but sometimes still functional protein, which

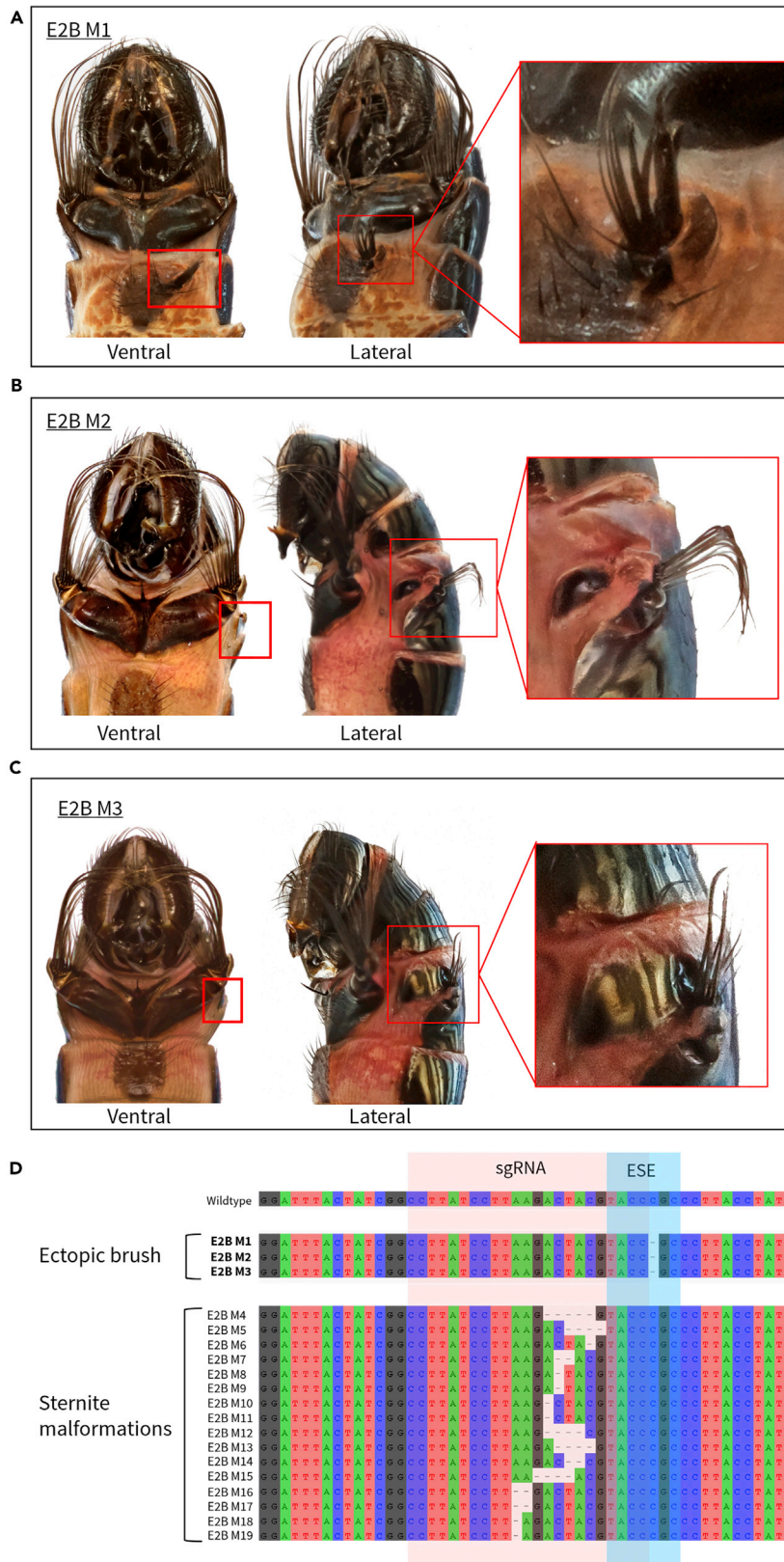


Figure 4. Ectopic Sternite Brush Phenotypes Obtained with Genome Editing of Exon 2

(A–D) (A) Ectopic mutant with ectopic brush on third ventral abdominal segment (E2BM1). (B and C) Ectopic mutants with ectopic brushes on the fourth dorsal abdominal segment (E2BM2 and E2BM3). (D) Sequences confirm that mutations underlying the ectopic brush phenotypes (E2BM1, E2BM2, E2BM3) lie within a predicted exonic splicing enhancer (ESE), whereas mutations underlying sternite malformation phenotypes (see Table S1) lie outside of the predicted ESE. The alignment is reverse complemented to display the putative ESE site sequence as predicted by ESEfinder 3.0 (Cartegni et al., 2003).

is in some instances over-expressed (Chang et al., 2007). It has also been recently shown in adenocarcinoma cells that CRISPR/Cas9-induced mutations lead to exon skipping (Mou et al., 2017).

Genome Editing at Exon 2 (sgRNA-2b) Results in Exon Skipping and the Production of an Altered *Dll* Protein with an Intact Homeodomain

We hypothesized that the ectopic phenotypes in sepsids may be gain-of-function mutants that resulted from an altered *Dll* protein that retains partial or full function. To test this, we investigated whether mutations in Exon 2 (sgRNA-2B) generate exon-skipped *Dll* transcripts in embryos. We injected two replicates of 160 embryos with Cas9 protein, and sgRNA-2B. RNA was extracted from the two mutant replicates (C1 and C2) as well as two wild-type replicates. RT-PCR was performed on 12-hr-old mutant and wild-type embryos. Primers were anchored in Exon 1 and Exon 3 of *Dll* (see Table S4 for primers). We found an alternatively spliced transcript lacking Exon 2 in both mutant embryo replicates, but not in the wild-type replicates (Figure 5).

Sanger sequencing of the shorter PCR product obtained from C1 and C2 confirms that Exon 2 was skipped. Based on sequence predictions, we find that with leaky scanning this exon-skipped transcript could produce an altered *Dll* protein with an intact homeodomain (Figure 6A). If translation of the exon-skipped transcript is initiated at the original start codon, the downstream homeodomain is disrupted, yielding a non-functional protein. However, examination of the *Dll* translation initiation site identified a putative alternative start site 1 bp immediately downstream of the Kozak sequence. Translation initiation at this alternative start codon would produce an exon-skipped protein with a functional homeodomain (Figure 6A). To show the feasibility of this mechanism, we performed an *in vitro* protein synthesis assay using a plasmid containing the *Dll*-coding sequence lacking Exon 2 (see Methods for details). We expressed a protein (>30 kDa) *in vitro* using the PURExpress kit (New England Biolabs) (Figure 6B). An analysis with the TripleTOF 5600 detected the presence of the bioinformatically predicted protein that is obtained only if the alternative initiation codon is utilized. The TripleTOF obtained peptides that correspond to Exon 1 of the predicted leaky-scanned protein, the intact *Dll* homeodomain, as well as Exon 5 (Figures 6A and S3).

These experiments suggest that exon skipping occurs and that the ectopic sternite brush phenotypes could arise from a change in expression of an altered *Dll* transcript with full or partial function. However, *Dll* expression was previously observed only in the developing fourth sternite brush during the late pupal stage (48 hr after puparium formation) (Bowsher and Nijhout, 2009), which could not explain the presence of ectopic brushes on the third abdominal segment as observed in mutant E2B M1. To discern whether the underlying predicted change in expression levels was a spatial gain of expression or a misregulation of an already expressed gene, we investigated *Dll* expression in the developing histoblast clusters in the late larval stage in *T. biloba* and *D. melanogaster*. RT-PCR was performed on dissected epidermal larval segments; the epidermis includes the histoblast clusters that eventually develop into the adult sternites and tergites. We found that *Dll* expression in *D. melanogaster* was detected in all abdominal segments as well as in the thoracic segment (Figure S5). To rule out any artifacts from imprecise dissections, another gene, Abdominal-B (*Abd-B*), was tested. As expected in *D. melanogaster*, *Abd-B* was only detected in the fifth to eighth abdominal segments. Similar to *D. melanogaster*, in *T. biloba* the RT-PCR results indicate that *Dll* is present in all abdominal segments in the larval stages (Figure S4 and Table S5).

Genome Editing of Another Putative ESE Site (sgRNA-2A) within Exon 2 Again Produces Both Gain and Loss Phenotypes

To test the hypothesis that specific mutations within ESE sites produce mutants with ectopic phenotypes, we designed a guide targeting another predicted ESE site within Exon 2 (sgRNA-2A, Table S1) and found

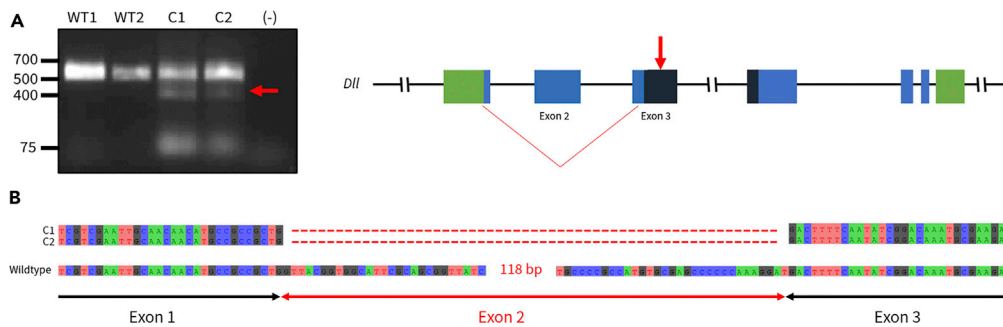


Figure 5. CRISPR/Cas9-Induced Deletions in Exonic Splicing Enhancer (ESE) of Exon 2 (sgRNA-2B) Generate Exon-Skipped *Dll* Transcripts

(A) Primers flanking sgRNA-2B were used to amplify cDNA obtained from the two mosaic mutant embryo replicates (C1 and C2) and wild-type embryos. C1 and C2 mosaic mutants produced a mixture of a short PCR product (~500 bp) and the wild-type PCR product (726 bp). (B) Sanger sequencing of the shorter PCR product obtained from C1 and C2 confirms that Exon 2 has been excluded; an altered *Dll* transcript is present in both replicates of Exon 2 mutant embryos. Sanger sequencing of the longer product yields a wild-type *Dll* sequence.

comparable results. We observed nine mutants with sternite malformations with one mutant exhibiting a complete loss of one-half of the fourth sternite appendage (E2A M2). Interestingly, we also observed one mutant male (E2A M1) with an ectopic fourth sternite brush: on the right half of the fourth sternite appendage, the third sternite is expanded, whereas the fourth sternite is misshapen and ends in two bristled lobes instead of the expected one (Figure 7A). Upon characterization of all the mutants using NGS, we observed that only the mutations underlying the ectopic brush mutant disrupted the targeted ESE site. The most abundant mutant haplotype was a single point deletion within the ESE site, whereas the second most abundant mutant haplotype was a 57-bp deletion that disrupts the targeted ESE site as well as an additional downstream putative ESE site. As predicted, the mutations underlying the loss and other sternite malformations lay outside of the ESE site. These results lend further support to the hypothesis that specific CRISPR/Cas9-induced mutations that disrupt ESE sites have the potential to yield ectopic phenotypes, either through an over-expression or a prolonged expression of an altered but functional *Dll* protein.

To discern if this exon-skipped transcript was exclusively the result of targeted genome editing at Exon 2 (sgRNA-2A), we performed targeted long-read isoform sequencing on Pacbio Sequel to qualitatively characterize the alternative splice forms of *Dll* present in both exon-skipped mutants and wild-type individuals. Using a guide targeting Exon 2, we injected 405 embryos and screened the surviving third instar larvae. RNA was extracted from 12 injected and 2 wild-type larvae and used to synthesize cDNA. Using an *in vitro* cleavage assay, 2 of the 12 larvae were identified as exon-skipped mutants (M4 and M6). We then designed *Dll*-specific tagged primers anchored in Exon 1 and Exon 7 (see Table S4 for tagged primer sequences) to amplify *Dll* splice forms, which were then sent in for Pacbio Sequel targeted isoform circular consensus sequencing. This generates a consensus sequence from multiple passes of a single circular molecule. The reads were analyzed using the Pacbio SMRT Link 5.1.0 analysis software (see Methods for parameters).

From the sequencing data, we identified three splice forms alongside the wild-type splice form (Figure 8). Splice forms B and C were detected in M6 and both wild-type larvae. However, splice form A, which excluded Exon 2, was only detected in the exon-skipped mutants, M4 and M6. These results suggest that the exon-skipped transcript (splice form A) does not naturally occur and is instead produced only when Exon 2 (sgRNA-2A) is disrupted with CRISPR/Cas9.

To test if changed expression levels of *Dll* can be detected in ectopic mutants, we carried out a quantitative PCR assay on injected mosaic mutant larvae despite the high risk of such an experiment yielding a false-negative result because (1) mosaic mutant larvae have a mixture of wild-type, mutant, and exon-skipped transcripts; (2) only mosaic mutants with a high proportion of wild-type cells are predicted to be viable;

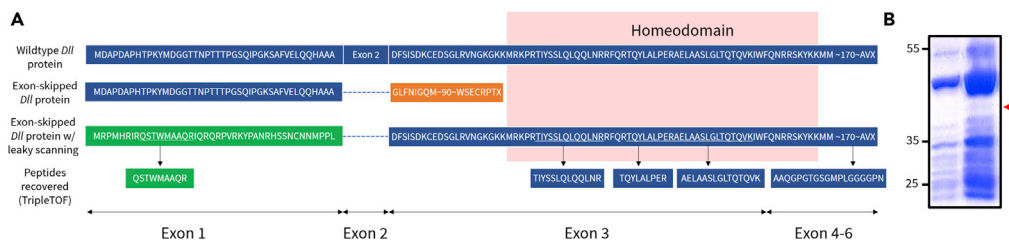


Figure 6. Protein Predictions

(A) The exon-skipped *Dll* transcript generates an altered protein with a disrupted homeodomain. However, with leaky scanning, the exon-skipped *Dll* transcript can generate an altered protein that recapitulates the wild-type protein sequence from Exon 3 onward with an intact homeodomain. Analysis with a TripleTOF 5600 recovered peptides that matched to the predicted “*Dll* protein under leaky scanning.”

(B) The *in vitro*-synthesized truncated *Dll* protein and control reaction were separated on a 10% SDS-polyacrylamide gel and visualized with Coomassie blue staining. The exon-skipped *Dll* transcript was translated into a >30-kDa protein product.

and (3) the natural expression levels of *Dll* at this stage are low. The results of the qPCR assay were inconclusive (see [Methods](#) for details).

DISCUSSION

The overall body plan of winged insects has remained remarkably conserved with regard to the position of appendages, which are restricted to the head, thorax, and posteriormost segments of the 11-segmented abdomen (genitalia). Occasional exceptions to this body plan are losses or reductions of structures, such as the reduction of maxillary and mandibular structures in *D. melanogaster* (Angelini and Kaufman, 2006). However, gains of articulated appendages, especially in the pregenital abdominal segments, are rare. Sepsids are one of the few exceptions (Hoch et al., 2014), having very recently evolved a novel abdominal appendage. This makes sepsids an attractive model system for understanding how a gene regulatory network is assembled for the development of novel appendages.

Morphological novelties are often hypothesized to arise from either existing or *de novo* genetic machinery (True and Carroll, 2002; Wagner and Lynch, 2010). Genes can either be co-opted along with their existing network or be assembled differently into a *de novo* network. In addition, novel phenotypes may also arise from the evolution of *de novo* or orphan genes. Recent studies have shown that the genetic architecture underlying morphological novelties in insects is more complex than expected; in some instances, a combination of both *de novo* genes and the co-option of an existing gene regulatory network underly a novel phenotype (Santos et al., 2017; Hilgers et al., 2018), whereas in others, existing gene regulatory networks are modified and/or partially co-opted (Hu et al., 2018; Moczek, 2009; Moczek and Rose, 2009; Glassford et al., 2015). We illustrate in this study another instance whereby an important gene in the appendage-patterning gene regulatory network, *Dll*, is co-opted in the development of a novel morphological structure: the fourth sternite brush.

Here, we show conclusively that *Dll* is necessary for the development of a novel abdominal appendage in *T. biloba*; disruptions in the homeodomain and in the coding region upstream lead to losses of the fourth sternite brush. We also observed malformed monomorphic sternites in both males and females, raising the question of how *Dll* fits into a gene regulatory network that patterns a sexually dimorphic trait. To obtain a better understanding of the underlying gene architecture responsible for building this morphological novelty, functional characterization of more appendage and sex-patterning genes (e.g., *doublesex*) would have to be carried out.

Moreover, we also reveal that specific deletions in Exon 2 can lead not only to the expected losses but also to unexpected gains of the novel fourth sternite brush. Through a detailed dissection of the upstream coding exon, we show that deletions in ESE sites can generate the ectopic phenotypes observed and go further to prove that the ensuing exon-skipped transcripts can be translated *in vitro* into an altered *Dll* protein that retains an intact homeodomain. These findings highlight how small modifications of *Dll* have the potential to generate very different phenotypes. This would be a single observation in a fly species if it were not

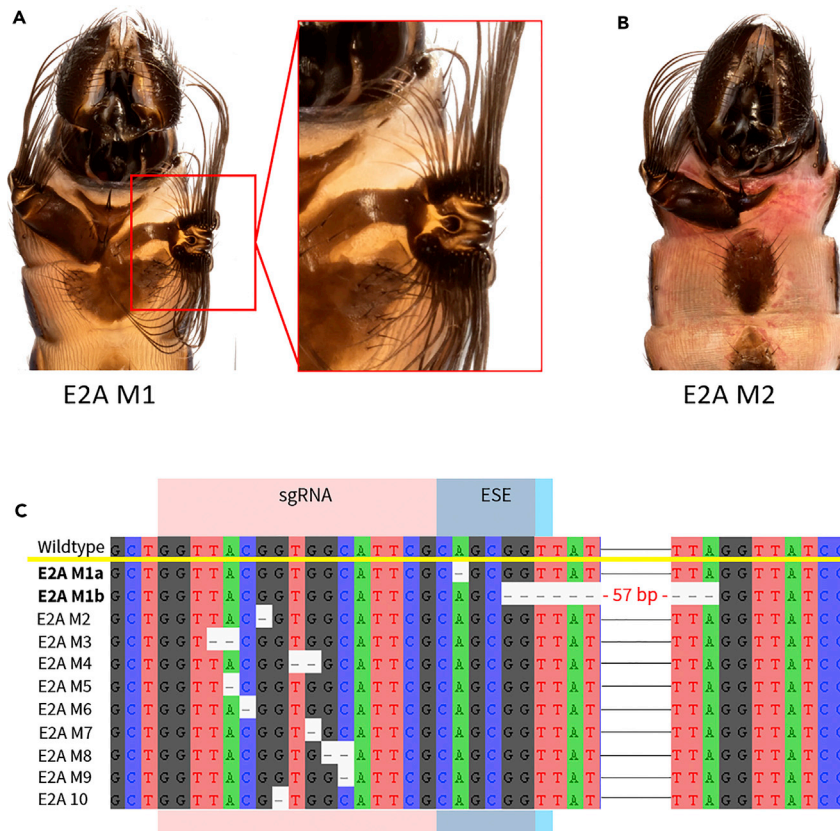


Figure 7. Mutant Phenotypes Obtained with Genome Editing of Second Putative ESE Site in Exon 2 (sgRNA-2A) (A–C) Mutant with ectopic brush on fourth ventral abdominal segment (E2A M1). (B) Mutant with loss of half of the fourth sternite brush (E2A M2). (C) Sequences confirm that mutations underlying the ectopic brush phenotype (E2A M1) lie within a predicted exonic splicing enhancer (ESE), whereas mutations underlying sternite malformation phenotypes lie outside of the predicted ESE. The two most abundant mutant haplotypes for E2A M1 are shown in this alignment (E2A M1a is a single-point deletion, whereas E2A M1b is a 57-bp deletion that disrupts this target ESE site as well as another downstream ESE site).

for the fact that a similarly diverse set of phenotypes can be generated by mutations in the same coding region in butterflies, which diverged from flies nearly 300 million years ago (Misof et al., 2014). In both sepsid flies and several species of butterflies (*V cardui* and *B. anynana*), disruption of the region upstream of the *Dll* homeodomain produces ectopic structures (Zhang and Reed, 2016; Connahs et al., 2017) and exon-skipped *Dll* transcripts (Connahs et al., 2017). Moreover, a comparative analysis across Holometabola reveals that the region of *Dll* immediately upstream of the homeodomain is highly conserved. The conserved nature of this protein region as well as the appearance of ectopic traits in two divergent lineages suggests that mutations at this conserved region may have had the potential to generate morphological variation for at least 300 million years. Although we find in *T. biloba* that the exon-skipped transcript does not occur naturally, further investigation into *B. anynana* and other holometabolan lineages might provide more insight into the possible role of this conserved region in the evolution and development of structural novelties.

Based on our results, we propose that *Dll* genome editing studies should target multiple exons and include the exon upstream of the homeodomain. Such screening may yield particularly interesting results for those species that have novel traits whose development involves *Dll*. Our study suggests that this gene may not only be important for the origin of novel traits but also has the potential for generating morphological diversity via splicing regulation. These findings also have implications beyond *Dll* as CRISPR/Cas9 is now extensively adopted for genome editing purposes from single cells to whole organisms. Future CRISPR/Cas9 studies should target multiple exons, particularly functional domains, to identify phenotypes generated by exon skipping. Bioinformatics tools should be also used to predict

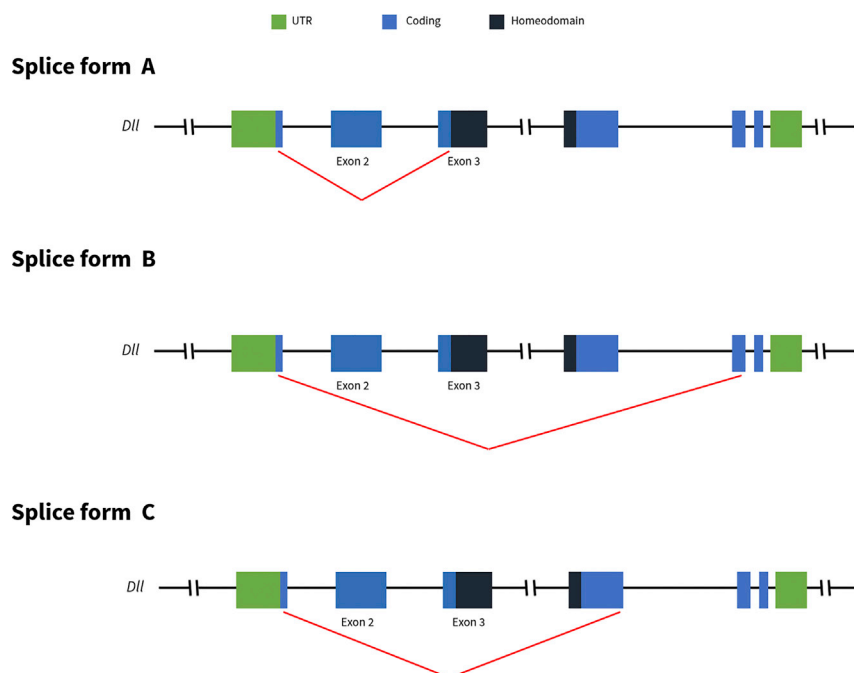


Figure 8. Alternative Splice Forms Identified from Pacbio Isoform Sequencing of Two Exon-Skipped Mutant Individuals (M4 and M6) and Two Wild-Type Individuals

Splice form A excludes Exon 2 and is found only in the two mutant individuals, M4 and M6. Splice form B, which excludes Exon 2 to Exon 4, is found in both wild-type individuals and M6. Splice form C, which excludes Exon 2, Exon 3, and part of Exon 4 is found in M6 and the two wild-type individuals.

ESE sites in potential target regions, which should either be avoided to reduce the chances of generating conflicting results or targeted with CRISPR/Cas9 to test whether gain-of-function mutations can be produced.

Limitations of Study

Our study suggests that deletions in ESE sites result in exon skipping and the development of ectopic structures. However, the process by which exon-skipped transcripts produce the ectopic structures remains unclear because quantifying gene expression of mutated cells within a mosaic mutant is difficult, i.e., we were not able to isolate the signal from mutant cells alone. We predict that the exon-skipped transcript is functional because the homeodomain is intact. However, *in vivo* tests for protein folding and functionality would be desirable.

METHODS

All methods can be found in the accompanying [Transparent Methods supplemental file](#).

DATA AND SOFTWARE AVAILABILITY

Most of the processed sequencing data files are available on a Mendeley database <https://doi.org/10.17632/ps3p7jnb5t.1>.

SUPPLEMENTAL INFORMATION

Supplemental Information includes Transparent Methods, five figures, and six tables and can be found with this article online at <https://doi.org/10.1016/j.isci.2018.11.036>.

ACKNOWLEDGMENTS

This work was supported by a Lee Kuan Yew Postdoctoral Fellowship grant (R-154-000-646-112) and an MOE AcRF Tier 2 grant (R-154-000-A62-112). The authors would like to thank Amrita Srivathsan and Ang

Yuchen for their assistance with bioinformatics and imaging, respectively. We also thank Zhang Yizhong and Lee Zheng Fen for their assistance with microinjections. We extend our gratitude to Mindy Tuan for providing us with the mating behavior of *Themira superba*, Dacotah Melicher for providing us with *Dll* scaffolds, Fong Siao Wan for her assistance with the RNA extractions and RT-PCR experiments, Antonia Monteiro and Heidi Connahs for the stimulating discourse, and Sunita Subramaniam, Lim Teck Kwang, Anjali Gupta, and Thorsten Wohland for assistance with the protein experiments. We would also like to thank Liou Yih-Cherng for feedback on the protein experiments. For help with our qPCR experiment, we would like to thank Hiong Kum Chew and Ip Yuen Kwong. We also thank Julia H. Bowsher for her assistance with the design of the RT-PCR experiments and her insightful feedback on the manuscript.

AUTHOR CONTRIBUTIONS

K.F.Y.S. and G.R. planned the study, performed most of the experiments, and wrote the paper with feedback from the other authors. K.F.Y.S., G.R., and A.S. performed the microinjection experiments, and G.R. conducted the imaging, characterization, and analysis of CRISPR/Cas9 mutants. K.F.Y.S. designed the guides for CRISPR experiments and performed the *in vitro* protein synthesis assay, reverse-transcriptase PCR, qPCR experiments, and alignments of *Dll* across Holometabola. G.R. performed the SDS protein gels and the ProteinPilot analysis. K.F.Y.S. designed the *Dll* isoform experiment, and K.F.Y.S. and G.R. processed and analyzed the results. R.M. supervised and supported the research; all authors discussed the results and provided comments for the manuscript.

DECLARATION OF INTERESTS

The authors declare no competing financial interests.

Received: August 8, 2018

Revised: November 26, 2018

Accepted: November 27, 2018

Published: December 21, 2018

REFERENCES

- Ang, Y. (2013). Modern Morphological Techniques and the Evolutionary Biology and Taxonomy of Sepsidae (Diptera), PhD thesis (National University of Singapore).
- Angelini, D.R., and Kaufman, T.C. (2006). Insect appendages and comparative ontogenetics. *Dev. Biol.* 286, 57–77.
- Arnout, L., Su, K.F.Y., Manoel, D., Minervino, C., Magriña, J., Gompel, N., and Prud'homme, B. (2013). Emergence and diversification of fly pigmentation through evolution of a gene regulatory module. *Science* 339, 1423–1426.
- Bowsher, J.H., Ang, Y., Ferderer, T., and Meier, R. (2013). Deciphering the evolutionary history and developmental mechanisms of a complex sexual ornament: the abdominal appendages of Sepsidae (Diptera). *Evolution* 67, 1069–1080.
- Bowsher, J.H., and Nijhout, H.F. (2007). Evolution of novel abdominal appendages in a sepsid fly from histoblasts, not imaginal discs. *Evol. Dev.* 9, 347–354.
- Bowsher, J.H., and Nijhout, H.F. (2009). Partial co-option of the appendage patterning pathway in the development of abdominal appendages in the sepsid fly *Themira biloba*. *Dev. Genes Evol.* 219, 577–587.
- Cartegni, L., Wang, J., Zhu, Z., Zhang, M.Q., and Krainer, A.R. (2003). ESEfinder: a web resource to identify exonic splicing enhancers. *Nucleic Acids Res.* 31, 3568–3571.
- Chang, Y.-F., Chan, W.-K., Imam, J.S., and Wilkinson, M.F. (2007). Alternatively spliced T-cell receptor transcripts are up-regulated in response to disruption of either splicing elements or reading frame. *J. Biol. Chem.* 282, 29738–29747.
- Cohen, S.M., and Jürgens, G. (1989). Proximal—distal pattern formation in *Drosophila*: cell autonomous requirement for Distal-less gene activity in limb development. *EMBO J.* 8, 2045–2055.
- Connahs, H., Tlili, S., van Creijl, J., Loo, T.Y.J., Banerjee, T., Saunders, T.E., and Monteiro, A. (2017). Disrupting different Distal-less exons leads to ectopic and missing eyespots accurately modeled by reaction-diffusion mechanisms. [bioRxiv](#).
- Glassford, W.J., Johnson, W.C., Dall, N.R., Smith, S.J., Liu, Y., Boll, W., Noll, M., and Rebeiz, M. (2015). Co-option of an ancestral hox-regulated network underlies a recently evolved morphological novelty. *Dev. Cell* 34, 520–531.
- Hilgers, L., Hartmann, S., Hofreiter, M., and von Rintelen, T. (2018). Novel genes, ancient genes, and gene co-option contributed to the genetic basis of the radula, a molluscan innovation. *Mol. Biol. Evol.* 35, 1638–1652.
- Hoch, H., Wessel, A., Asche, M., Baum, D., Beckmann, F., Bräunig, P., Ehrig, K., Mühlethaler, R., Riesemeier, H., Staude, A., et al. (2014). Non-sexual abdominal appendages in adult insects challenge a 300 million year old bauplan. *Curr. Biol.* 24, R16–R17.
- Hong-Xiang, L., Cartegni, L., Zhang, M.Q., and Krainer, A.R. (2001). A mechanism for exon skipping caused by nonsense or missense mutations in BRCA1 and other genes. *Nat. Genet.* 27, 55–58.
- Hu, Y., Schmitt-Engel, C., Schwirz, J., Stroehlein, N., Richter, T., Majumdar, U., and Bucher, G. (2018). A morphological novelty evolved by co-option of a reduced gene regulatory network and gene recruitment in a beetle. *Proc. Biol. Sci.* 285.
- Khila, A., Abouheif, E., and Rowe, L. (2012). Function, developmental genetics, and fitness consequences of a sexually antagonistic trait. *Science* 336, 585–589.
- Melicher, D., Torson, A.S., Dworkin, I., and Bowsher, J.H. (2014). A pipeline for the de novo assembly of the *Themira biloba* (Sepsidae: Diptera) transcriptome using a multiple k-mer length approach. *BMC Genomics* 15, 188.
- Misof, B., Liu, S., Meusemann, K., Peters, R.S., Donath, A., Mayer, C., Frandsen, P.B., Ware, J., Flouri, T., Beutel, R.G., et al. (2014). Phylogenomics resolves the timing and pattern of insect evolution. *Science* 346, 763–767.
- Moczek, A.P. (2009). On the origins of novelty and diversity in development and evolution: a case

study on beetle horns. *Cold Spring Harb. Symp. Quant. Biol.* 74, 289–296.

Moczek, A.P., and Rose, D.J. (2009). Differential recruitment of limb patterning genes during development and diversification of beetle horns. *Proc. Natl. Acad. Sci. U S A* 106, 8992–8997.

Mou, H., Smith, J.L., Peng, L., Yin, H., Moore, J., Zhang, X.-O., Song, C.-Q., Sheel, A., Wu, Q., Ozata, D.M., et al. (2017). CRISPR/Cas9-mediated genome editing induces exon skipping by alternative splicing or exon deletion. *Genome Biol.* 18, 108.

Santos, M.E., Le Bouquin, A., Crumière, A.J.J., and Khila, A. (2017). Taxon-restricted genes at the origin of a novel trait allowing access to a new environment. *Science* 358, 386–390.

Toga, K., Hojo, M., Miura, T., and Maekawa, K. (2012). Expression and function of a limb-patterning gene *Distal-less* in the soldier-specific morphogenesis in the nasute termite *Nasutitermes takasagoensis*. *Evol. Dev.* 14, 286–295.

True, J.R., and Carroll, S.B. (2002). Gene co-option in physiological and morphological evolution. *Annu. Rev. Cell Dev. Biol.* 18, 53–80.

Wagner, G.P., and Lynch, V.J. (2010). Evolutionary novelties. *Curr. Biol.* 20, R48–R52.

Wang, J., Hamilton, J.I., Carter, M.S., Li, S., and Wilkinson, M.F. (2002). Alternatively spliced TCR mRNA induced by disruption of reading frame. *Science* 297, 108–110.

Zhang, L., and Reed, R.D. (2016). Genome editing in butterflies reveals that *spalt* promotes and *Distal-less* represses eyespot colour patterns. *Nat. Commun.* 7, 11769.

ISCI, Volume 10

Supplemental Information

**CRISPR/Cas9 deletions in a conserved exon
of *Distal-less* generates gains and losses in a
recently acquired morphological novelty in flies**

Gowri Rajaratnam, Ahiraa Supeinthiran, Rudolf Meier, and Kathy F.Y. Su

1 **Supplemental Information**

2

3 **CRISPR/Cas9 deletions in a conserved exon of *Distal-less* generates gains and losses in a**
4 **recently acquired morphological novelty in flies.**

5

6 **Authors:**

7

8 Gowri Rajaratnam¹, Ahiraa Supeinthiran³, Rudolf Meier^{1,2*} and Kathy F.Y. Su^{1*}

9 ¹ Department of Biological Sciences, National University of Singapore, Singapore

10 ² Lee Kong Chian Natural History Museum, Singapore

11 ³ University of Toronto Scarborough, Canada

12 *corresponding author

13

14

15 **Transparent Methods**

16 **Fly cultures**

17 *Themira biloba* fly cultures were kept at a constant temperature of 23 °C with a 12-hour light
18 and dark cycle and maintained on a diet of duck and bovine dung.

19 **Preparation of guide RNAs**

20 Three CRISPR guide RNAs targeting Exon 2 and Exon 3 (homeodomain) were designed for
21 *T. biloba*. *T. biloba* assembled transcriptome was downloaded from NCBI, Accession number
22 PRJNA218740 (Melicher et al., 2014). Using CLC Genomics Workbench we searched for
23 *Dll* transcript sequences within the *T. biloba* transcriptome using BLASTn against *D.*
24 *melanogaster Dll*. Using CLC Genomics Workbench we then designed guides targeting Exon
25 2 and Exon 3 of *T. biloba Dll*. We searched for regions that contained GGN₁₉NGG. The
26 guides were screened for off-target effects using a blastn query against the assembled *T.*
27 *biloba* transcriptome (Melicher et al., 2014). Specifically, for sgRNA-2B, this search did not
28 find any 100% off-target matches. However, it did identify three hits with a hit-length of 13
29 bp and E-values around 1E-3. Further investigation of these hits reveal that they do not flank
30 a PAM site and so are unlikely to result in off-target effects (Supplementary table 2).

31 The single guide RNA (sgRNA) templates were synthesised artificially using **gBlocks® Gene**
32 **Fragments (Integrated DNA Technologies)**. Following *in vitro* transcription of the gblocks
33 DNA template with a T7 polymerase (New England Biolabs), the sgRNAs were purified
34 using the TURBO DNase kit followed by the Qiagen RNeasy kit. *In vitro* Cas9 cleavage
35 assays were then carried out to test the guide's ability to cut the target DNA fragment in the
36 presence of Cas9 protein (PNAbio).

37 **Microinjection**

38 Eggs were extracted from the egg-laying substrate after 4 hours, rinsed gently, aligned onto a
39 coverslip, and covered with a thin layer of oil to prevent desiccation. 1ul of 1ug/ul Cas9
40 protein (PNAbio) was mixed with 1ul of 1ug/ul of sgRNA and injected into the posterior of
41 the eggs using a 76mm needle. Needles were pulled fresh with a Sutter P-97 Flaming/Brown
42 type micropipette puller. To overcome the lethality of a *Dll* knockdown in early
43 embryogenesis (Cohen and Jürgens, 1989), the protocol was optimized to reduce the number

44 of mosaic mutant cells generated by injecting 4-hour old embryos with a reduced volume of
45 the sgRNA/Cas9 complex.

46 The injected eggs were then rinsed thoroughly and kept in a moist chamber for 24 hours. The
47 emerging larvae were then picked out and placed into petri dishes of bovine dung to develop.
48 After 8-10 days, the pupae were recovered and left to develop in a moist chamber. The
49 emerging adults were allowed to completely sclerotize for 3 days before they were screened
50 for mutations. The mutant individuals were then preserved in 70% ethanol for imaging and
51 DNA extraction. Images were obtained using a Visionary Digital Imaging system.

52 **Genotyping of Mutations**

53 QuickExtract (Bioline) solution was used to extract gDNA from mutant tissue dissected from
54 the vicinity of affected structure. Extracted DNA was used to amplify the gene region of
55 interest (~200 bp fragment). The tarsi of a wildtype *T. biloba* male were dissected and used as
56 a control for this experiment.

57 PCR products were cleaned up with SureClean and sent for Illumina Miseq (2x301bp)
58 sequencing at 10,000x coverage (the read count and coverage for each sample is listed in
59 Supplementary table 3).. These mutations were mostly small deletions within the guide
60 sequence. To ensure that the mutations observed were not an artefact of PCR or sequencing
61 error, 3 PCR replicates (with tagged primers, Supplementary table 4) were carried out for all
62 mutants. The reads for all three replicates were processed separately and combined after
63 ascertaining that the three most abundant reads for each were identical. This combined
64 dataset was then used for the quantification of the read count and proportions of mutant
65 haplotypes for each specimen.

66 The DNA reads were then recovered using an in-house pipeline: the sequences were merged
67 using PEAR(Zhang et al., 2014) and demultiplexed using an in-house script (Meier et al.,
68 2016) to generate a fasta file for each PCR product/specimen. The reads were aligned using
69 MAFFT v7.0 (Kato et al., 2002). Once aligned, the sequences were submitted to the ‘DNA
70 to haplotype collapser and converter’ Fabox tool.(Villesen, 2007) This generates a table of
71 haplotypes and read counts as well as a summary of all the haplotypes observed. The three
72 most abundant haplotypes were recorded (see Supplementary table 3). The most abundant
73 mutant haplotype for each specimen was used for downstream alignments and comparisons.
74 The results were also confirmed with CRISPresso (Pinello et al., 2016) (window size set to
75 30 bp and sequence homology for an HDR occurrence set to 98%). Bioinformatics analysis

76 for ESE sites were performed using ESEfinder (v 3.0)(Cartegni et al., 2003). We used the
77 weighted matrix values for SRSF1, the human homolog of the Drosophila SF2/ASF at the
78 threshold of 1.956(Smith et al., 2006).

79 **Control Injections**

80 To rule out off-target effects and injection artefacts, 1004 embryos were injected with 500ng
81 of Cas9 alone. Note that the control injections were used to train students in the
82 microinjection technique and as such, the mortality for the control injections is high overall
83 due to mechanical damage. No mutants of any type were observed for the surviving adults.
84 Adults from control injections were genotyped and no mutations were observed.

85 **Exon-skipping**

86 In order to detect if exon skipping was occurring when Exon 2 was targeted, RNA was
87 extracted from two independent replicates of 160 injected embryos (C1 and C2) as well as
88 two wildtype replicates using TRIzol (Invitrogen). The RNA was transcribed into cDNA
89 using the ProtoScript II First Strand cDNA synthesis kit (New England Biolabs). The gene
90 region of interest was then amplified. The same volume of product was loaded onto a 1%
91 agarose gel for both the wildtype and mutant replicates. A shorter band (~ 400bp) was
92 observed for only C1 and C2 and not the wildtype replicates (Fig.5A). The shorter band was
93 then sent for Sanger sequencing, where a transcript lacking Exon 2 was found.

94 **Protein analysis**

95 PCR was used to generate the template needed for *in vitro* protein synthesis. Primers specific
96 to the start and stop codons of *Dll* coding sequence were used to add specific adaptor
97 sequences (see PURExpress manual and supplementary table 4) to the *Dll* coding sequence
98 lacking Exon 2. A T7 promoter and ribosome binding site were added to the upstream of the
99 start of *Dll* translation and a 35-mer loop structure was added to the 3' of *Dll* coding
100 sequence (See PURExpress manual and supplementary table 4 for primer sequences). This
101 PCR product was purified using the Qiagen PCR purification kit and used as a template for *in*
102 *vitro* protein synthesis with the PURExpress kit (New England Biolabs). Both the *Dll*
103 template as well as a control reaction with no template were set-up and processed in the same
104 way. 8ul of this synthesised protein product was run out on an SDS-PAGE gel (10% Mini-
105 PROTEAN® TGX™ Precast Gel) at 120V for 90 minutes, along with the control. The >30
106 kDa band, representing the synthesized *Dll* protein, was excised from the gel and sent for

107 analysis on the Triple TOF 5600 (Ab SCIEX). Unfortunately, we noticed that although the
108 same amount of the reaction was loaded onto the gel, the control reaction appeared fainter
109 than the reaction with the *Dll* template.

110 As an additional measure to rule out the possibility that the >30kDa band was simply not
111 observed in the fainter control, we excised out the corresponding area in the control gel lane
112 and sent it in for mass spectrometry analysis as well.

113 The Mass Spectra raw data was searched against the NCBI *D. melanogaster* protein database
114 and the *E. coli* database supplemented with the *Dll* predicted protein sequence for *Themira*
115 *biloba* with ProteinPilot® v4.5 (Revision: 1656; Paragon Algorithm: 4.5.0.0, 1654). Searches
116 were run as thorough identification searches, specifying tryptic digestion and cys-alkylation
117 (Iodoacetamide). For the *Dll* protein sample, peptides were found with strong matches to an
118 alternative initiation codon as well as to the homeodomain and Exon 4 (Supplementary
119 Figure 3). No confident peptide matches were found for the analogous control sample
120 (supplementary file in Mendeley resource).

121 ***Distal-less* isoform characterisation**

122 In order to qualitatively characterise the alternative splice forms of *Dll* present in both mutant
123 and wildtype individuals, targeted long-read isoform circular consensus
124 sequencing (Gonzalez-Garay, 2016) was conducted for 4 individuals. 405 embryos were
125 injected with sgRNA-2A (targeting the second ESE site within Exon 2). After 7 days, total
126 RNA and DNA was isolated from 12 injected 3rd instar larvae using TRIzol® Reagent
127 (Invitrogen). cDNA was synthesised using the ProtoScript II First Strand cDNA synthesis kit
128 (New England Biolabs) for each of these individuals and an in-vitro cleavage assay was
129 performed to identify the mutant specimens. Two individuals (M4 and M6) were observed
130 with mutations and exon skipping.

131 Similarly, RNA was extracted and used for cDNA synthesis for two wildtype 3rd instar larvae
132 (WT1 and WT2). Primers were designed within the *Dll* locus to amplify and capture *Dll*
133 specific splice forms (Supplementary Table 4). 5' phosphorylated forward primers were
134 designed in *Dll* exon 1 (5' UTR) and reverse 16bp-tagged primers were designed for *Dll* exon
135 7 (3' UTR). A 16bp tag unique to each specimen was attached to the 3' end of the reverse
136 primer so as to identify the two wildtype and two mutant sequences (see Supplementary table
137 4 for primer and tag sequences). The PCR products were purified with Sureclean and sent in
138 for Pacbio Sequel circular consensus sequencing with a library insert size of 2kb.

139 Pacbio IsoSeq files were error-corrected and converted into CCS reads; We performed 10
140 minimum passes with a minimum predicted accuracy of 0.9 using the PacBio SMRT analysis
141 software (v5.1.0). The analysis generated 225,740 CCS reads with a median CCS read length
142 between 1200 – 1249 bp (see Supplementary Figure 5 for results statistics).

143 The reads were then demultiplexed using Geneious with a 100% stringency match to primer
144 and tag sequences. The demultiplexed sequences were then filtered for low read length (<
145 500bp) yielding 18194 reads for M4, 124385 reads for M6, 13422 reads for WT1 and 18817
146 reads for WT2. For each individual, the reads were collapsed into haplotypes using the ‘DNA
147 to Haplotype converter’ tool in FaBox (Villesen, 2007). Haplotypes with read counts below
148 0.5% of the total count were discarded. The remaining haplotypes were aligned using
149 MAFFT v7.0 and then analysed in Aliview to identify alternative splice forms (alignment
150 files in Mendeley resource).

151 **Distal-less expression in developing histoblast clusters**

152 To determine if *Dll* was naturally expressed in the 3rd abdominal segment where an ectopic
153 sternite brush was observed, RNA was extracted from dissected epidermal tissues of 3rd instar
154 larvae. The epidermis of the thoracic segment and the abdominal segments (8 abdominal
155 segments for *D. melanogaster* and 7 abdominal segments for *T. biloba*) were dissected for 5
156 wildtype 3rd instar larvae for both *T. biloba* and *D. melanogaster*. RNA was extracted for
157 each segment and cDNA was synthesised. RT PCR for *Dll* was carried out for each segment
158 to check for *Dll* expression in the late larval stages.

159 The same was done for *D. melanogaster*, which served as a control for the RT-PCR
160 experiment. RT- PCR for an additional gene, Abdominal-B, was also carried out in *D.*
161 *melanogaster* as a control to rule out the presence of any artefacts from the epidermal
162 dissections. All PCR products were then PCR purified and sent in for sanger sequencing to
163 confirm the correct products were amplified (results in Supplementary Table 5,
164 Supplementary Figure 4).

165 **Distal-less alignment across Holometabola**

166 A protein search performed on NCBI using the following search terms “Distal-less[All
167 Fields] AND (“Mandibulata”[Organism] OR Mandibulata[All Fields])” yielded 467 protein
168 sequences. This dataset was filtered for sequences that: were not Distal-less, had no
169 homeodomain, were incomplete or of poor quality. Sequences belonging to Coleoptera,

170 Lepidoptera, Diptera and Hymenoptera were extracted from the filtered dataset and aligned
171 with MAFFT v7.0(Katoh et al., 2002) and visualised in Aliview (Larsson, 2014).

172 **Quantitative PCR**

173 We injected embryos with both Cas9 and the guide targeting Exon 2 and compared
174 expression levels to control embryos that were injected with Cas9 alone. We let embryos
175 develop into first instar larvae. All control larvae were individually extracted for RNA using
176 Trizol. All treatment larvae were first genotyped to confirm presence of mutations in Exon 2
177 using the T7 endonuclease kit (New England Biolabs). RNA from mutant larvae was then
178 used for cDNA synthesis to generate template for qPCR. The Forkhead transcription factor
179 (Mnf) gene was used as a housekeeping gene. We utilised a customised TaqMan gene
180 expression assay with primers nested within the homeodomain and with a probe
181 complementary to the homeodomain. The expression levels were not significantly different
182 between wildtype and mutant larvae. However, note that CRISPR/Cas9 generates mosaic
183 mutants that consist mostly of wildtype cells and mutants that survive are likely to only have
184 small amounts of mutant cells. This makes it difficult to disentangle expression levels
185 between wildtype mRNA from wildtype cells and exon-skipped transcripts of mutant cells.
186 With naturally low *Dll* expression (Ct value > 30), a lack of significant expression difference
187 is inconclusive.

188 **Data availability**

189 Most of the processed sequencing data files are available on a Mendeley database (DOI:
190 10.17632/ps3p7jnb5t.1). However, for pre-filtered/processed files and other data, please
191 contact Rajaratnam, G. For the in-house bioinformatics script, please contact Meier, R.

192 **References**

- 193 CARTEGNI, L., WANG, J., ZHU, Z., ZHANG, M. Q. & KRAINER, A. R. 2003. ESEfinder:
194 a web resource to identify exonic splicing enhancers. *Nucleic Acids Research*, 31,
195 3568-3571.
- 196 COHEN, S. M. & JÜRGENS, G. 1989. Proximal—distal pattern formation in *Drosophila*:
197 cell autonomous requirement for Distal-less gene activity in limb development. *The*
198 *EMBO Journal*, 8, 2045-2055.
- 199 GONZALEZ-GARAY, M. L. 2016. Introduction to Isoform Sequencing Using Pacific
200 Biosciences Technology (Iso-Seq). In: WU, J. (ed.) *Transcriptomics and Gene*
201 *Regulation*. Dordrecht: Springer Netherlands.
- 202 KATOH, K., MISAWA, K., KUMA, K.-I. & MIYATA, T. 2002. MAFFT: a novel method
203 for rapid multiple sequence alignment based on fast Fourier transform. *Nucleic Acids*
204 *Research*, 30, 3059-3066.

205 LARSSON, A. 2014. AliView: a fast and lightweight alignment viewer and editor for large
206 datasets. *Bioinformatics*, 30, 3276-3278.

207 MEIER, R., WONG, W., SRIVATHSAN, A. & FOO, M. 2016. \$1 DNA barcodes for
208 reconstructing complex phenomes and finding rare species in specimen-rich samples.
209 *Cladistics*, 32, 100-110.

210 MELICHER, D., TORSON, A. S., DWORKIN, I. & BOWSER, J. H. 2014. A pipeline for
211 the de novo assembly of the *Themira biloba* (Sepsidae: Diptera) transcriptome using a
212 multiple k-mer length approach. *BMC Genomics*, 15, 188.

213 PINELLO, L., CANVER, M. C., HOBAN, M. D., ORKIN, S. H., KOHN, D. B., BAUER, D.
214 E. & YUAN, G.-C. 2016. Analyzing CRISPR genome-editing experiments with
215 CRISPResso. *Nat Biotech*, 34, 695-697.

216 SMITH, P. J., ZHANG, C., WANG, J., CHEW, S. L., ZHANG, M. Q. & KRAINER, A. R.
217 2006. An increased specificity score matrix for the prediction of SF2/ASF-specific
218 exonic splicing enhancers. *Hum Mol Genet*, 15, 2490-508.

219 VILLESSEN, P. 2007. FaBox: an online toolbox for fasta sequences. *Molecular Ecology*
220 *Notes*, 7, 965-968.

221 ZHANG, J., KOBERT, K., FLOURI, T. & STAMATAKIS, A. 2014. PEAR: a fast and
222 accurate Illumina Paired-End reAd mergeR. *Bioinformatics*, 30, 614-620.

223

224

225

226

227

228

229

230

231

232

233

234

235

236

237

238

239

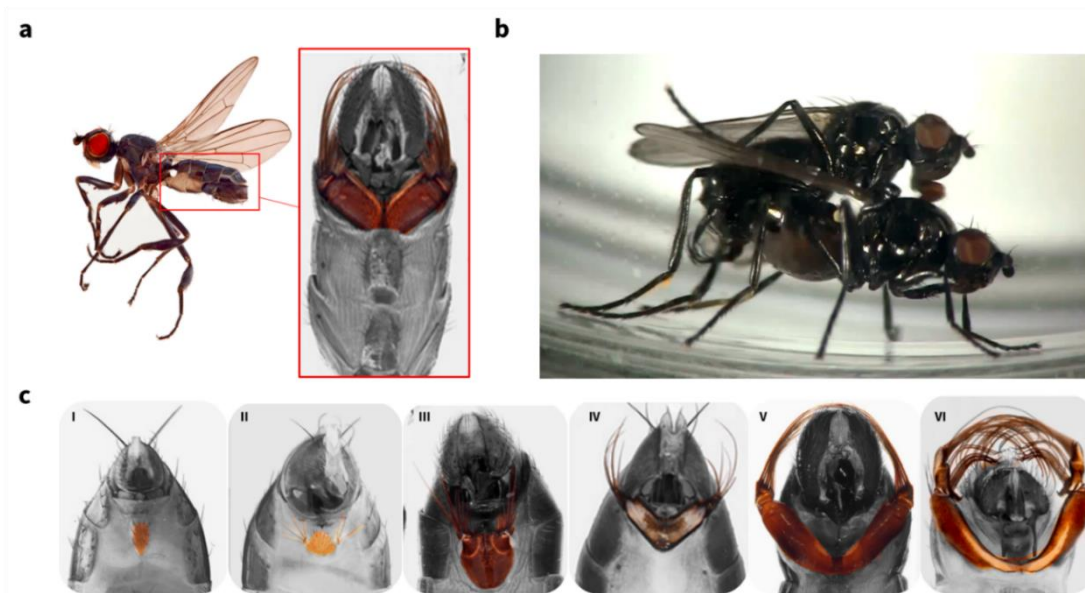
240

241

242 **Figures**

243

244



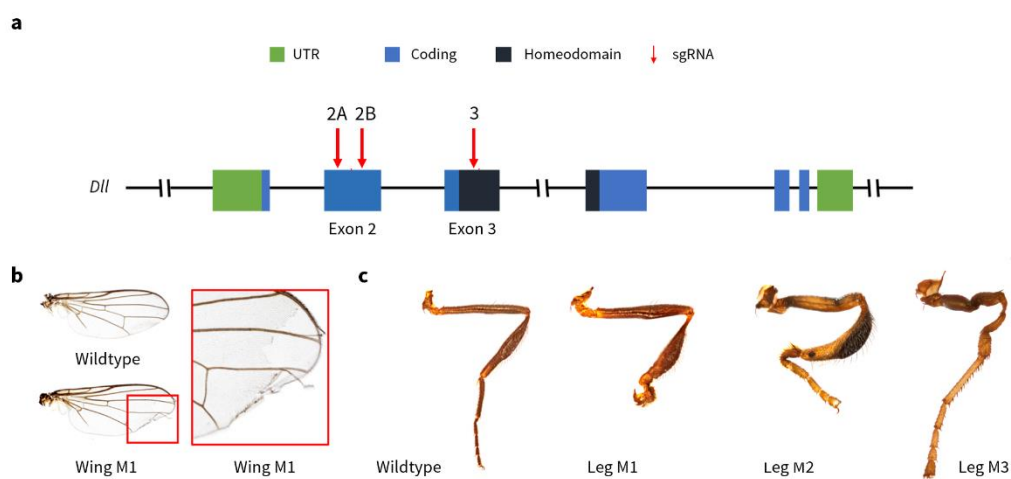
245

246 **Figure 1**

247

248

249



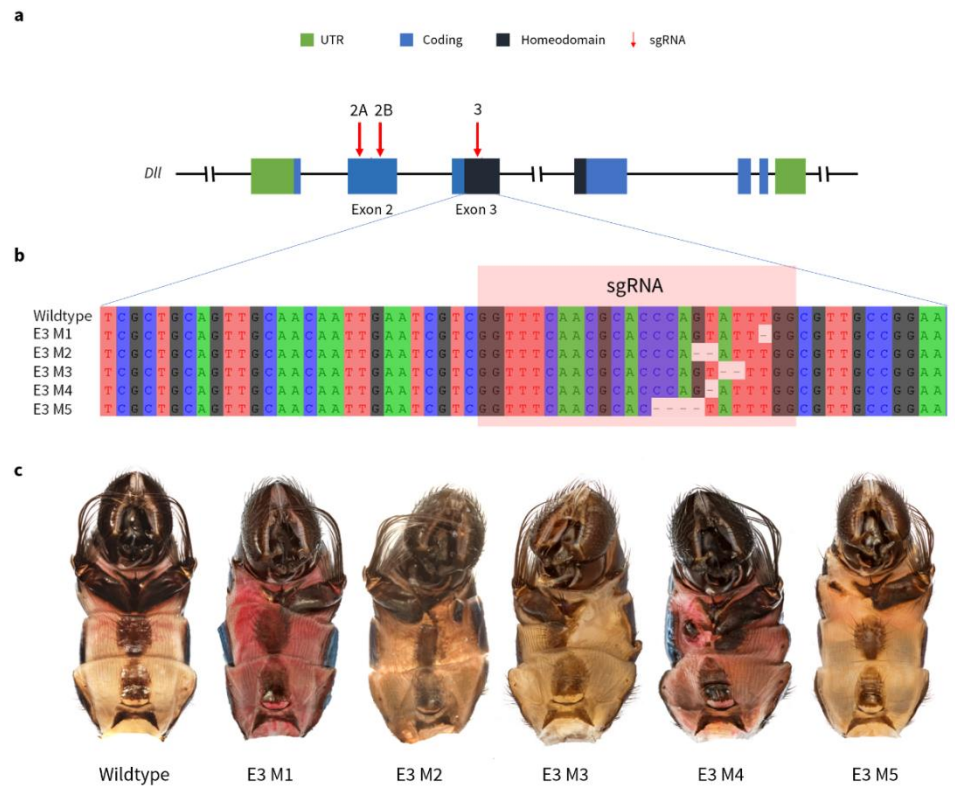
250

251 **Figure 2**

252

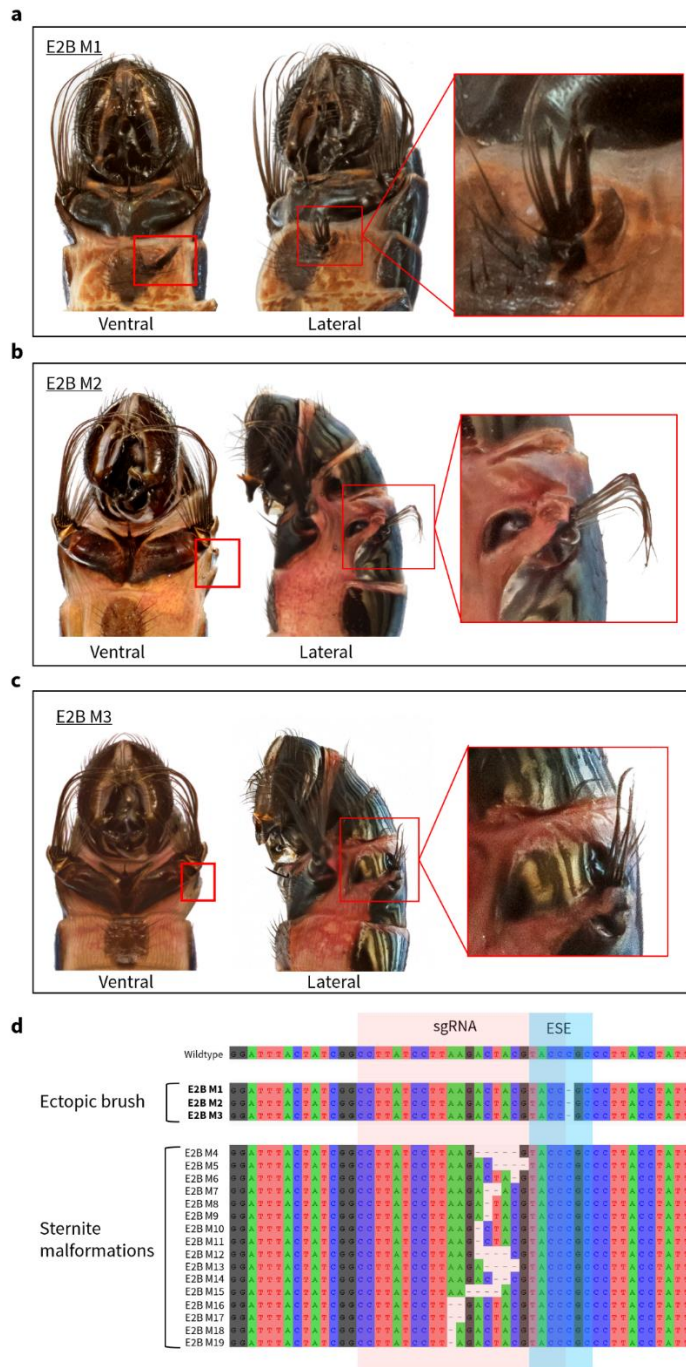
253

254
255



256
257
258

Figure 3.

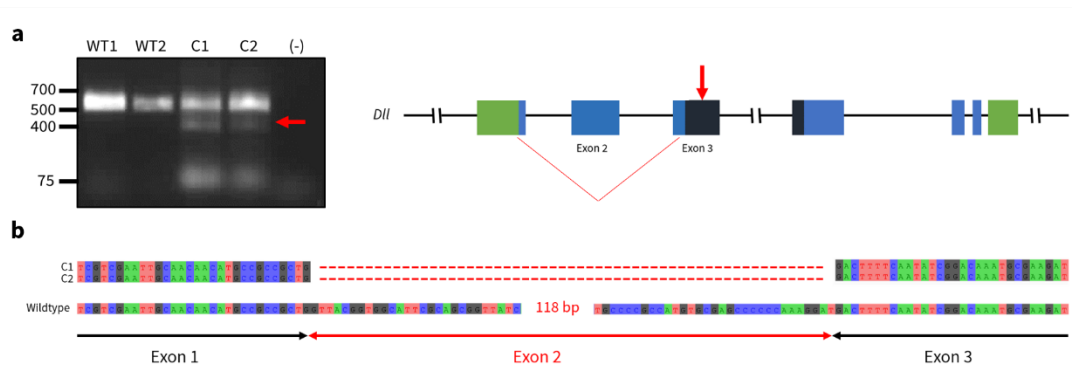


259

260 **Figure 4**

261

262



263

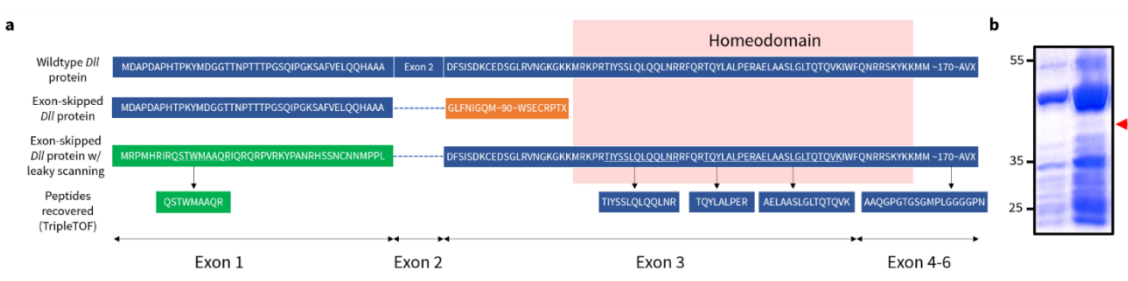
264

Figure 5

265

266

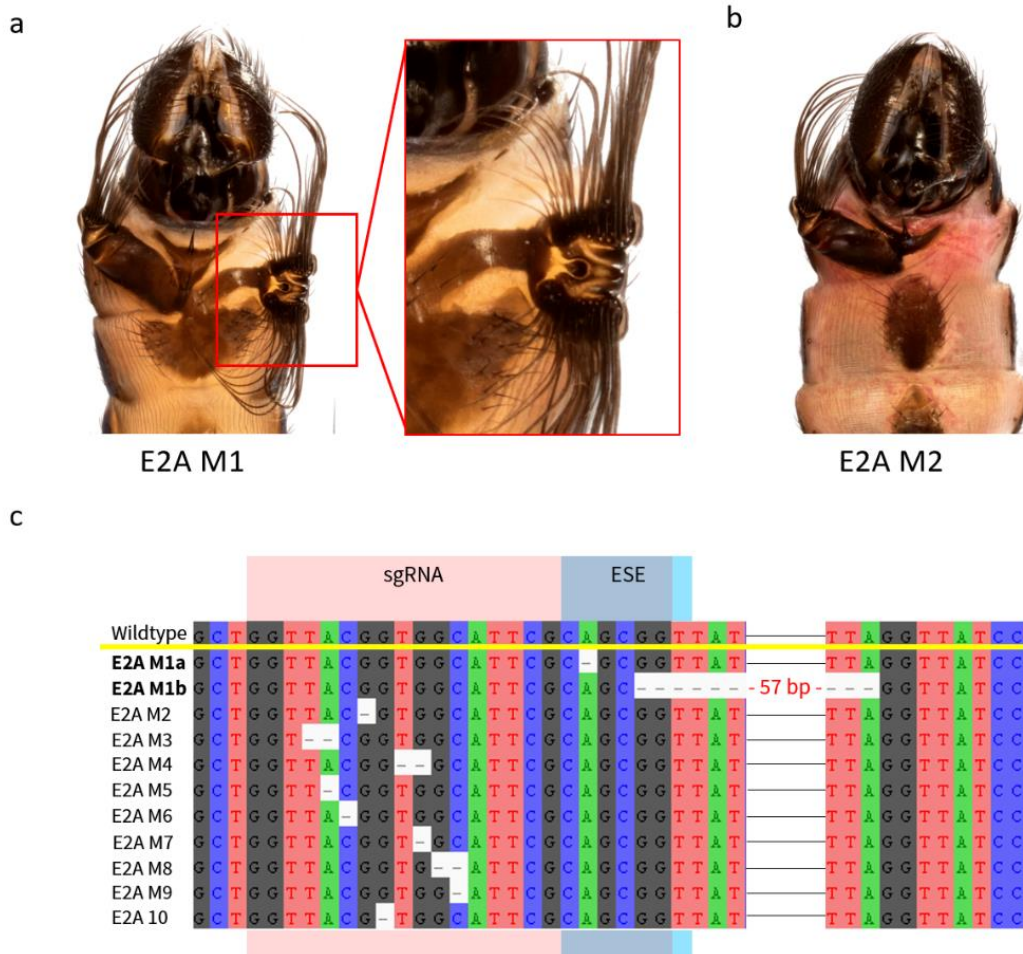
267



268

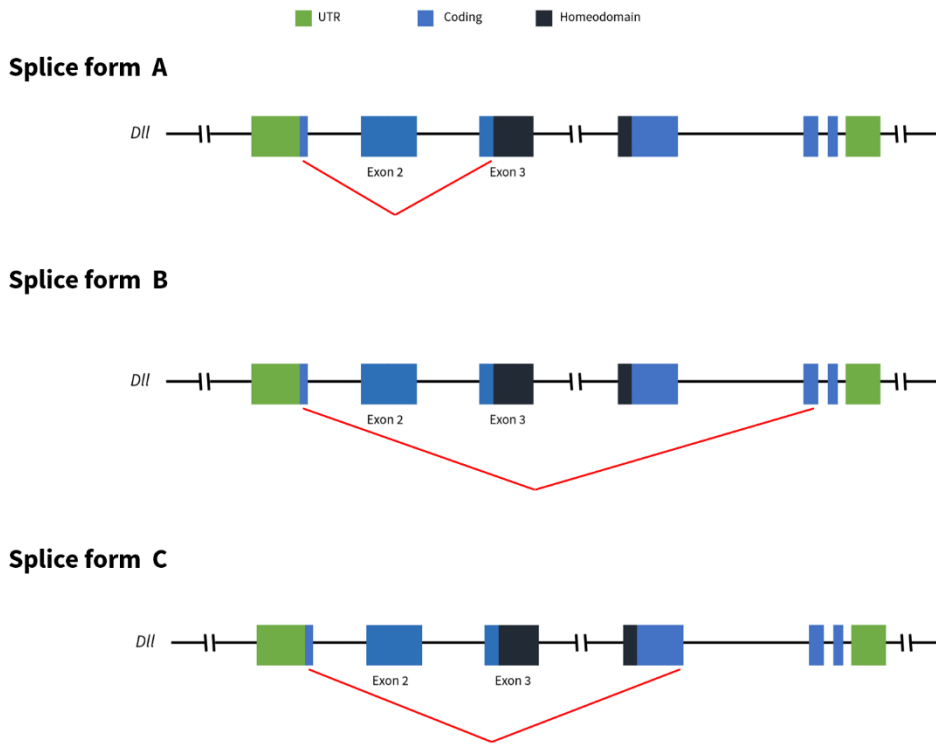
269

Figure 6



270

271 **Figure 7**



272

273 **Figure 8**

274

275

276 Tables

277

278 **Table 1.**

279

	Injected eggs	Larvae	Adults	Mutants			
				Leg/Wing	Sternite malformations	Ectopic structures	Others (e.g. clasper malformations)
Exon 2 (sgRNA 2A)	1715	605	151	1	8	1	0
Exon 2 (sgRNA 2B)	4631	957	363	8	29	3	6
Exon 3 (sgRNA3)	4003	1187	261	1	21	0	2
Control	1004	153	109	0	0	0	0

280 **Supplementary information**

281

282 **Supplementary Table 1.** Summary of ESEfinder search with Matrix values for SRSF1
 283 (human homolog for SF2/ASF) with threshold of 1.956. The ESE motif present in Exon 2
 284 sgRNA-2B is highlighted in bold while the ESE motif used to design sgRNA-2A is italicized.
 285 Related to Figure 4.

Sequence ID	Motif	Position on Exon 2	Motif	Score
gi 654231031 gb GBGG01003309.1	SRSF1	100	cgcccat	2.21734
<i>gi 654231031 gb GBGG01003309.1 </i>	<i>SRSF1</i>	<i>17</i>	<i>cagcggg</i>	<i>4.39195</i>
gi 654231031 gb GBGG01003309.1	SRSF1	49	gtcagga	3.28514
gi 654231031 gb GBGG01003309.1	SRSF1	75	cgcagtg	2.69094
gi 654231031 gb GBGG01003309.1	SRSF1	15	cgcagcg	2.23323
gi 654231031 gb GBGG01003309.1	SRSF1	169	caaagga	3.67496

286

287 **Supplementary Table 2.** Summary of blastn results. Related to Figure 4.

Query	Number of HSPs	Lowest E-value	Accession (E-value)	Greatest identity %	Greatest HSP length	Greatest bit score	Sequence overlap with guide %
gi 654231031 gb GBGG01003309.1 (<i>Themira biloba</i> DII)	1	1.38661E-06	sgRNA-2B	100	20	32.7626	100
gi 654228759 gb GBGG01004492.1	1	0.0066504	sgRNA-2B	100	13	21.9569	65
gi 654228161 gb GBGG01004814.1	1	0.00242708	sgRNA-2B	100	13	21.9569	65
gi 654223893 gb GBGG01007092.1	1	0.00259143	sgRNA-2B	100	13	21.9569	65

288

289 **Supplementary Table 3.** Summary of read counts for mutant haplotypes. The 3 most
 290 dominant mutant haplotypes per individual are recorded here. The dominant haplotype (in
 291 bold) per individual is used for downstream analyses. See separate excel document. Related
 292 to Figure 2, 3, 4 and 7.

293

294

295

296

297 **Supplementary Table 4.** Primer sequences. Tags are in lower case. Related to Figure 2, 3, 4,
 298 5, 7 and 8.

Purpose	Name	Primer sequence (5' → 3')
Characterisation of homeodomain mutants	Dll_sgrna12_F1	cagtctgGACAAATGCGAAGATTCTGG
Characterisation of homeodomain mutants	Dll_sgrna12_F2	catgggaGACAAATGCGAAGATTCTGG
Characterisation of homeodomain mutants	Dll_sgrna12_F3	tcacgtaGACAAATGCGAAGATTCTGG
Characterisation of homeodomain mutants	Dll_sgrna12_F4	tggccaGACAAATGCGAAGATTCTGG
Characterisation of homeodomain mutants	Dll_sgrna12_F5	aacctgtGACAAATGCGAAGATTCTGG
Characterisation of homeodomain mutants	Dll_sgrna12_F6	cttggttGACAAATGCGAAGATTCTGG
Characterisation of homeodomain mutants	Dll_sgrna12_R1	cagtctgCTGCGTTTGTGTTAGGCCCA
Characterisation of homeodomain mutants	Dll_sgrna12_R2	catgggaCTGCGTTTGTGTTAGGCCCA
Characterisation of homeodomain mutants	Dll_sgrna12_R3	tcacgtaCTGCGTTTGTGTTAGGCCCA
Characterisation of homeodomain mutants	Dll_sgrna12_R4	tggccaCTGCGTTTGTGTTAGGCCCA
Characterisation of homeodomain mutants	Dll_sgrna12_R5	aacctgtCTGCGTTTGTGTTAGGCCCA
Characterisation of homeodomain mutants	Dll_sgrna12_R6	cttggttCTGCGTTTGTGTTAGGCCCA
Characterisation of Exon 2 mutants	Dll_sgrna4_F1	aacctgtTACGGTGGCATTTCGCAGCGGT TATC
Characterisation of Exon 2 mutants	Dll_sgrna4_F2	agaagtgTACGGTGGCATTTCGCAGCGG TTATC
Characterisation of Exon 2 mutants	Dll_sgrna4_F3	cggttatTACGGTGGCATTTCGCAGCGGT TATC
Characterisation of Exon 2 mutants	Dll_sgrna4_F4	gtacactTACGGTGGCATTTCGCAGCGGT TATC
Characterisation of Exon 2 mutants	Dll_sgrna4_F5	gtgatgaTACGGTGGCATTTCGCAGCGG TTATC
Characterisation of Exon 2 mutants	Dll_sgrna4_F6	cttggttTACGGTGGCATTTCGCAGCGGT TATC
Characterisation of Exon 2 mutants	Dll_sgrna4_R1	aacctgtGGGCTCGCACATGGCGGG
Characterisation of Exon 2 mutants	Dll_sgrna4_R2	agaagtgGGGCTCGCACATGGCGGG
Characterisation of Exon 2 mutants	Dll_sgrna4_R3	cggttatGGGCTCGCACATGGCGGG
Characterisation of Exon 2 mutants	Dll_sgrna4_R4	gtacactGGGCTCGCACATGGCGGG

Characterisation of Exon 2 mutants	Dll_sgrna4_R5	gtgatgaGGGCTCGCACATGGCGGG
Characterisation of Exon 2 mutants	Dll_sgrna4_R6	cttggttGGGCTCGCACATGGCGGG
Characterisation of ESE mutants	Dll_intron1_F1	aacctgtGTTGTGCCTCCAAGGATTTCATAC
Characterisation of ESE mutants	Dll_intron1_F2	agaagtg GTTGTGCCTCCAAGGATTTCATAC
Characterisation of ESE mutants	Dll_intron1_F3	cggttat GTTGTGCCTCCAAGGATTTCATAC
Characterisation of ESE mutants	Dll_intron1_F4	gtacact GTTGTGCCTCCAAGGATTTCATAC
Characterisation of ESE mutants	Dll_intron1_F5	gtgatga GTTGTGCCTCCAAGGATTTCATAC
Characterisation of ESE mutants	Dll_intron1_F6	cttggtt GTTGTGCCTCCAAGGATTTCATAC
Characterisation of ESE mutants	Dll_sgrna4_R1	aacctgtGGGCTCGCACATGGCGGG
Characterisation of ESE mutants	Dll_sgrna4_R2	agaagtgGGGCTCGCACATGGCGGG
Characterisation of ESE mutants	Dll_sgrna4_R3	cggttatGGGCTCGCACATGGCGGG
Characterisation of ESE mutants	Dll_sgrna4_R4	gtacactGGGCTCGCACATGGCGGG
Characterisation of ESE mutants	Dll_sgrna4_R5	gtgatgaGGGCTCGCACATGGCGGG
Characterisation of ESE mutants	Dll_sgrna4_R6	cttggttGGGCTCGCACATGGCGGG
Amplification of <i>Dll</i> in <i>Drosophila melanogaster</i>	Dmel_Dll_F2	CCGATAAGTGCGAGGACTCCGG
Amplification of <i>Dll</i> in <i>Drosophila melanogaster</i>	Dmel_Dll_R	CTGCGTTTTCGCTGAGGCCCA
Amplification of <i>Abd-B</i> in <i>Drosophila melanogaster</i>	Dmel_ABDB_44_2_F	CCCACCTACTCCTCGCCAGGCGG
Amplification of <i>Abd-B</i> in <i>Drosophila melanogaster</i>	Dmel_ABDB_57_1_R	TCCACTCGTGCAGTCCGGGATTGGGC
Shortened reverse primer with lower Tm for cycle sequencing of <i>Drosophila melanogaster</i> Abd-B amplicon	Dmel_ABDB_57_1_SEQ_R	TCCACTCGTGCAGTCCGGGATT
Amplification of <i>Dll</i> in <i>Themira biloba</i>	DLL Exon 2 sgRNA4 F	TAC GGT GGC ATT CGC AGC GGT TAT C
Amplification of <i>Dll</i> in <i>Themira biloba</i>	DLL Exon 2 sgRNA4 R	CAC ATG GCG GGG CAT AAC TGC CTA AAT G

314

315

316

317

318

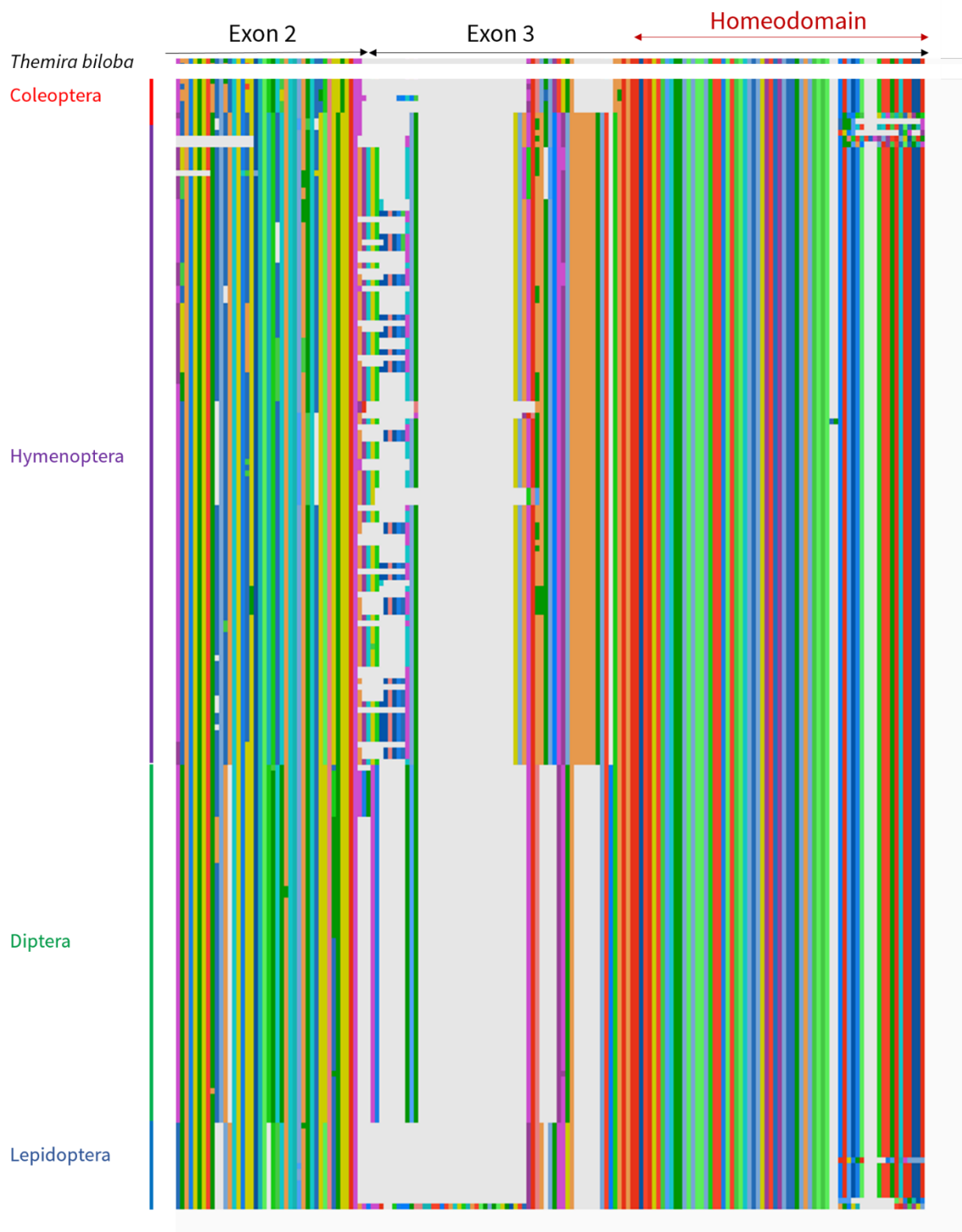
319

320



321

322 **Supplementary Figure 1.** Deletions in *Dll* Exon 2 produce mosaic mutant (E2B M8) with
323 loss of the 4th sternite brush. Related to Figure 4.



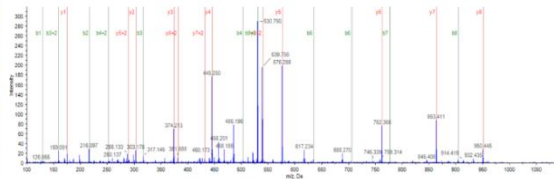
324

325 **Supplementary Figure 2.** Alignment of *Distal-less* protein sequences across holometabola.
 326 Alignment in fasta format is provided in the Mendeley resource. Related to Figure 4.

327

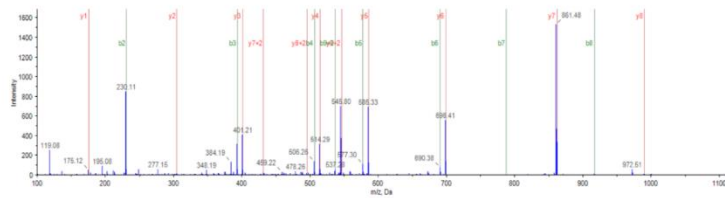
a

Residue	b	b+2	y	y+2
Q	129.0659	66.0366	1078.5098	539.7588
S	216.0979	108.5526	950.4513	475.7293
T	317.1458	159.0784	863.4192	432.2133
W	503.2249	252.1161	782.3716	381.8894
M	634.2654	317.6363	576.2922	288.6488
A	705.3025	353.1549	445.2518	223.1295
A	776.3396	388.6734	374.2146	187.6110
Q	904.3982	452.7027	303.1775	152.0924
R	1050.4993	530.7633	175.1190	88.0631



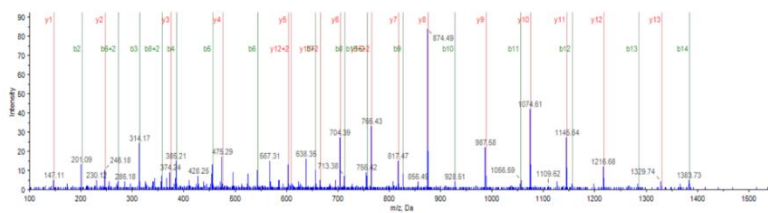
b

Residue	b	b+2	y	y+2
T	102.0550	51.5311	1090.5891	545.7982
Q	230.1135	115.5604	989.5415	495.2744
Y	393.1789	197.0921	861.4829	431.2451
L	506.2609	253.6341	698.4196	349.7134
A	577.2980	289.1527	588.3355	293.1714
L	690.3821	345.6947	514.2984	257.6529
P	787.4349	394.2211	401.2143	201.1108
E	916.4775	458.7424	304.1615	152.5844
R	1072.5785	536.7929	175.1190	88.0631



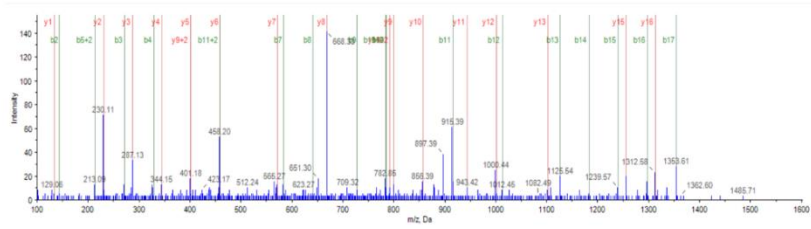
c

Residue	b	b+2	y	y+2
A	72.0444	36.5258	1529.8533	766.4303
E	201.0870	101.0471	1458.8162	729.9118
L	314.1710	157.5892	1329.7736	665.3905
A	385.2082	193.1077	1216.6896	608.8484
A	456.2453	228.6263	1145.6525	573.3299
S	543.2773	272.1423	1074.6154	537.8113
L	656.3614	328.6843	967.5833	494.2963
G	713.3828	357.1961	874.4993	437.7533
L	826.4669	413.7371	817.4778	409.2425
T	927.5146	464.2609	704.3937	352.7005
Q	1055.5732	528.2902	603.3461	302.1787
T	1156.6208	578.8141	475.2975	238.1474
Q	1294.6794	647.8433	374.2398	187.6236
V	1383.7478	692.3775	246.1812	123.5942
K	1511.8428	756.4259	147.1128	74.0600



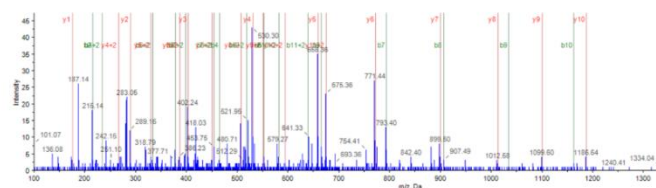
d

Residue	b	b+2	y	y+2
A	72.0444	36.5258	1562.7278	791.8676
A	143.0815	72.0444	1511.6907	756.3490
Q	271.1401	136.0737	1440.6536	720.8304
G	328.1615	164.5844	1312.5990	656.8012
P	425.2143	213.1108	1255.5736	628.2904
G	482.2368	241.6215	1158.5208	579.7640
T	583.2835	292.1454	1101.4990	551.2533
G	640.3049	320.6581	1000.4517	500.7296
S	727.3369	364.1721	943.4302	472.2187
G	784.3584	392.6820	868.3982	438.7027
M	915.3889	458.2931	799.3767	400.1920
F	1012.4517	506.7295	688.3362	334.6717
L	1125.5357	563.2715	571.2836	286.1454
G	1182.5572	591.7822	458.1994	229.6033
G	1239.5786	620.2930	401.1779	201.0928
L	1296.6001	648.8037	346.1565	172.5818
Q	1353.6216	677.3144	289.1350	144.0711
P	1410.6431	725.8408	230.1135	115.5804
N	1564.7173	782.8823	133.0688	67.0340



e

Residue	b	b+2	y	y+2
T	102.0550	51.5311	1093.8489	542.4281
I	215.1398	108.0731	1482.8013	731.9043
Y	378.2023	189.6048	1348.7172	675.3622
S	485.2344	233.1398	1196.6539	593.8208
S	582.2665	276.6300	1099.6276	548.3148
L	685.3085	333.9788	1012.5888	506.7985
Q	793.4090	397.2062	899.9587	450.2565
L	906.4931	453.7682	771.4472	386.2272
Q	1034.5517	517.7796	658.3631	328.8852
Q	1182.6183	591.8088	530.3045	265.8559
L	1275.6843	638.3688	402.2459	201.6296
N	1389.7373	695.3723	295.1679	148.3048
R	1545.8384	773.4228	175.1190	88.0631



328

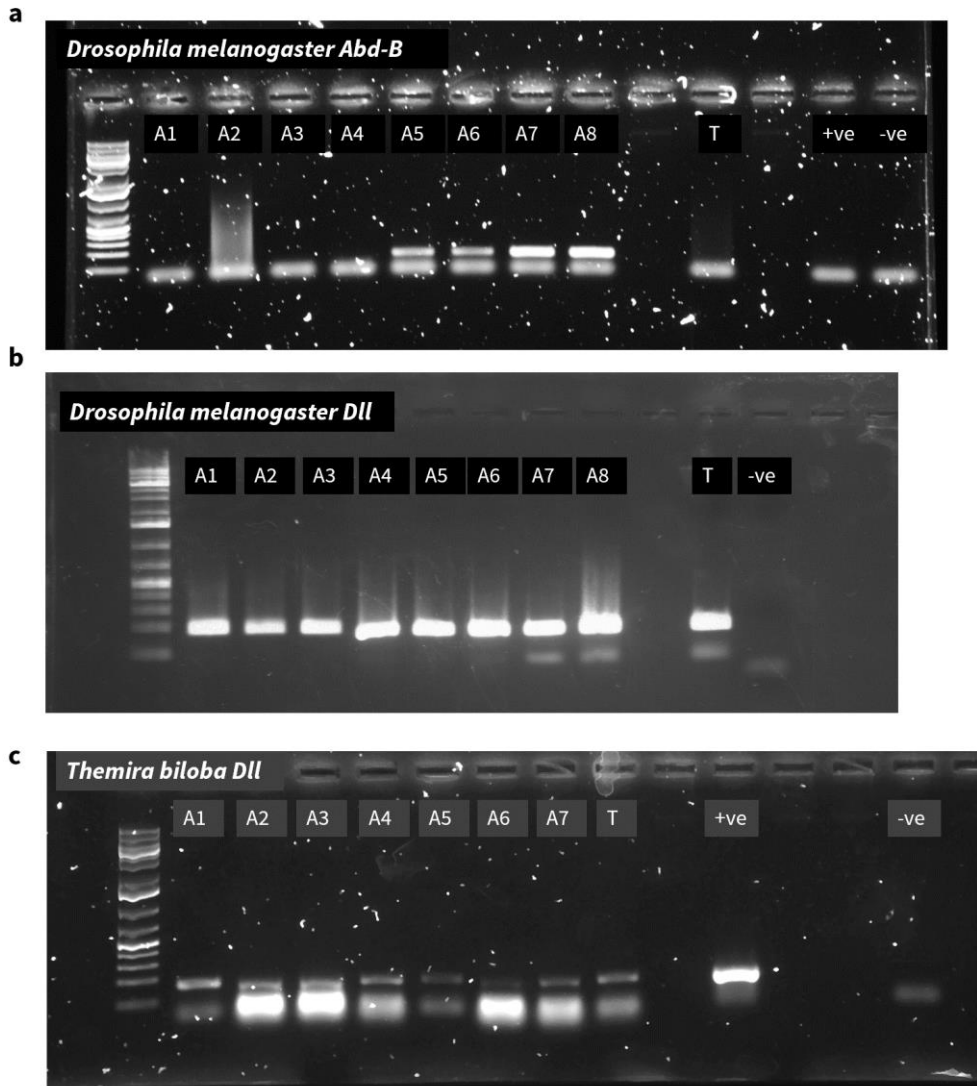
329 **Supplementary Figure 3.** Fragmentation evidence for *Dll* peptides recovered from
 330 ProteinPilot. (a) Fragment ion mass values and peptide peak intensity for ‘QSTWMAAQR’, a
 331 peptide matching to an alternative initiation codon (b), (c), (d) and (e) Fragment ion mass
 332 values and peptide peak intensity for peptides matching to *Dll* homeodomain. Related to
 333 Figure 6.

334

335

336

337

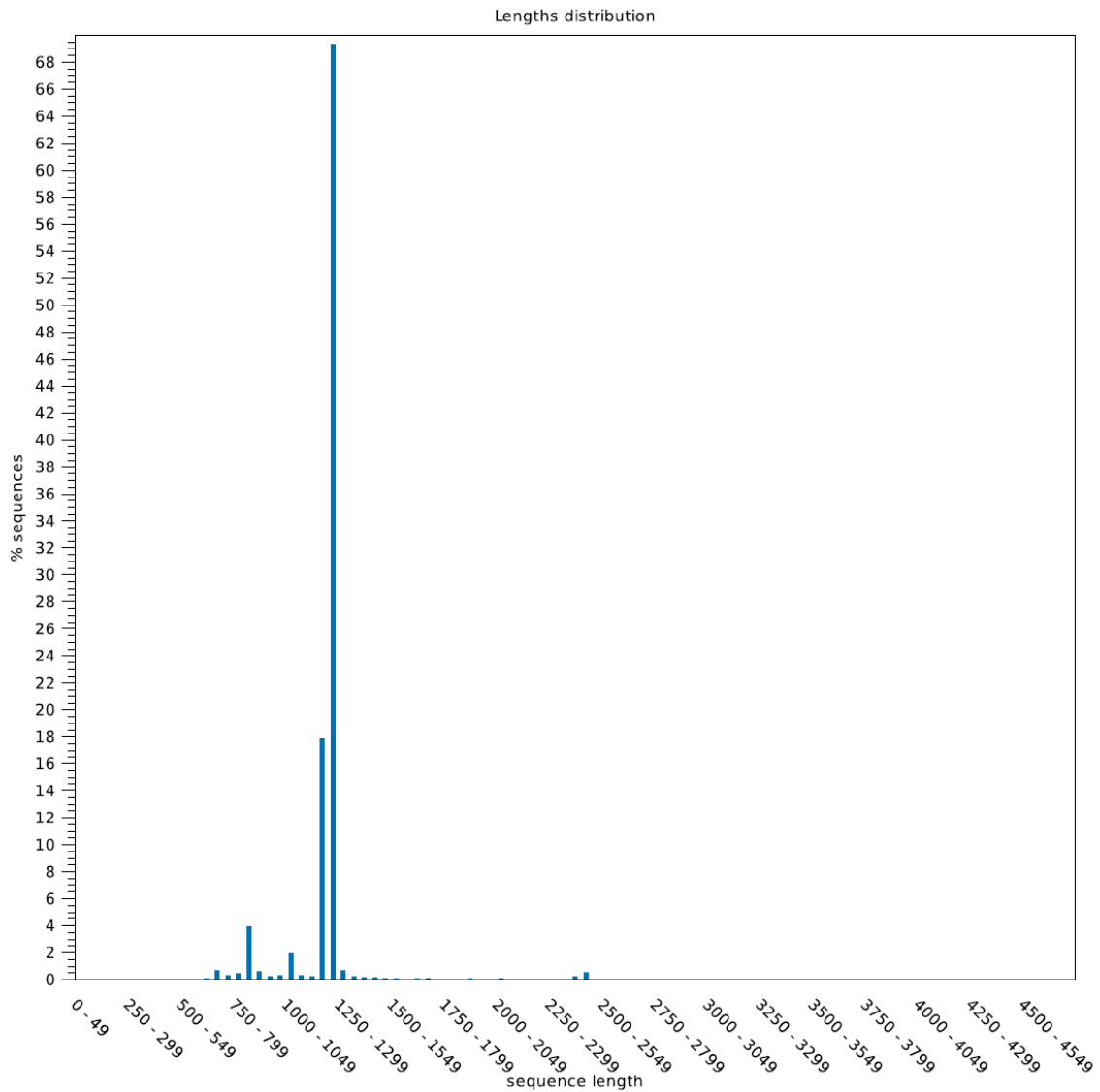


338

339 **Supplementary Figure 4.** RT-PCR results to determine *Dll* expression in late larval
340 epidermal tissues. *Drosophila melanogaster* was used as a control. Primers for this
341 experiment are found in Supplementary Table 5. Identity of amplified products were
342 confirmed with sanger sequencing (results in Supplementary Table 6). A1-A8: Tissue from
343 the respective abdominal epidermal segments. T: Tissue from the thoracic epidermal
344 segment. (a) In the control, *D.melanogaster*, Abd-B is present and amplified in the 5th – 8th
345 abdominal segments as expected. (b) *Dll* is present and amplified in all 8 abdominal segments
346 in *D.melanogaster* (c) *Dll* is present and amplified in all 7 abdominal segments in *Themira*
347 *biloba*. Related to Figure 7.

348

349
350
351
352



353
354

355 **Supplementary Figure 5.** Read length distribution of Pacbio Iseq error-corrected reads (10
356 minimum passes with a minimum predicted accuracy of 0.9) using the PacBio SMRT
357 analysis software (v5.1.0). The analysis generated 225,740 CCS reads with a median CCS
358 read length between 1200 – 1249 bp. Related to Figure 8.

359
360

361

362

363

364

365

366

367